

Forecasting range shifts of a dioecious plant species under climate change

Jacob K. Moutouama ^{*1}, Aldo Compagnoni², and Tom E.X. Miller¹

¹Program in Ecology and Evolutionary
Biology, Department of BioSciences, Rice University, Houston, TX USA

²Institute
of Biology, Martin Luther University Halle-Wittenberg, Halle, Germany; and
German Centre for Integrative Biodiversity Research (iDiv), Leipzig, Germany

Running header: Forecasting range shifts

Keywords: climate change, demography, forecasting, matrix projection model, mechanistic models, sex ratio, range limits

Submitted to: *Ecology letters* (Letter)

Data accessibility statement: All data (Miller and Compagnoni, 2022a) used in this paper are publicly available. Should the paper be accepted, all computer scripts supporting the results will be archived in a Zenodo package, with the DOI included at the end of the article. During peer review, our data and code are available at <https://github.com/jmoutouama/POAR-Forecasting>.

Conflict of interest statement: None.

^{*}Corresponding author: jmoutouama@gmail.com

1 Abstract

2 Rising temperatures and extreme drought events associated with global climate change have
3 triggered an urgent need for predicting species response to climate change. Currently, the vast
4 majority of theory and models in population biology, including those used to forecast biodiver-
5 sity responses to climate change ignore the complication of sex structure. To address this issue,
6 we developed two contrasting climate-driven matrix projection models (MPMs), one that ac-
7 count for sex structure and another one that does not account for sex structure. The MPMs were
8 built from demographic data of a dioecious species (Texas bluegrass), past and future climate
9 (different carbon gas emission scenarios). Both models predict females demographic advantage
10 (higher vital rate) over males. Climate change assuming moderate carbon emission has no neg-
11 ative impact on population viability. However, high carbon emission will likely alter population
12 viability in dioecious species and will induce a niche and range shift in the Northern edge of the
13 current range. We demonstrated that tracking only one sex could lead to an underestimation
14 of the impact of climate change on dioecious species. Overall, our work provides a framework
15 for predicting the impact of global warming on species using population demography.

¹⁶ Introduction

¹⁷ Rising temperatures and extreme drought events associated with global climate change are
¹⁸ leading to increased concern about how species will become redistributed across the globe
¹⁹ under future climate conditions (Bertrand et al., 2011; Gamelon et al., 2017; Smith et al., 2024).
²⁰ Dioecious species (most animals and many plants) might be particularly vulnerable to the
²¹ influence of climate change because they often display skewed sex ratios that are generated or
²² reinforced by sexual niche differentiation (distinct responses of females and males to shared cli-
²³ mate drivers) (Tognetti, 2012). Accounting for such a niche differentiation within a population
²⁴ is a long-standing challenge in accurately predicting which sex will successfully track environ-
²⁵ mental change and how this will impact population viability and range shifts (Gissi et al., 2023;
²⁶ Jones et al., 1999). The vast majority of theory and models in population biology, including
²⁷ those used to forecast biodiversity responses to climate change, ignore the complication of sex
²⁸ structure (Ellis et al., 2017; Pottier et al., 2021). As a result, accurate forecasts of colonization-
²⁹ extinction dynamics for dioecious species under future climate scenarios are limited.

³⁰ Species's range limits, when not driven by dispersal limitation, should generally reflect
³¹ the limits of the ecological niche (Lee-Yaw et al., 2016). For most species, niches and geographic
³² ranges are often limited by climatic factors including temperature and precipitation (Sexton
³³ et al., 2009). Therefore, any substantial changes in the magnitude of these climatic factors in a
³⁴ given location across the range could impact population viability, with implications for range
³⁵ shifts based on which regions become more or less suitable (Davis and Shaw, 2001; Pease
³⁶ et al., 1989). Forecasting range shifts for dioecious species is complicated by the potential for
³⁷ each sex to respond differently to climate variation (Morrison et al., 2016; Pottier et al., 2021).
³⁸ Populations in which males are rare under current climatic conditions could experience low
³⁹ reproductive success due to sperm or pollen limitation that may lead to population decline in
⁴⁰ response to climate change that disproportionately favors females (Eberhart-Phillips et al., 2017).
⁴¹ In contrast, climate change could expand male habitat suitability (e.g. upslope movement),
⁴² which might increases seed set for pollen-limited females and favor range expansion (Petry
⁴³ et al., 2016). Although the response of species to climate warming is an urgent and active area
⁴⁴ of research, few studies have disentangled the interaction between sex and climate drivers
⁴⁵ to understand their combined effects on population dynamics and range shifts.

⁴⁶ Our ability to track the impact of climate change on the population dynamics of
⁴⁷ dioecious plants and the implication of such impact on range shift depends on our ability
⁴⁸ to build mechanistic models that take into account the spatial and temporal context in which
⁴⁹ sex specific response to climate change affects population viability (Czachura and Miller, 2020;
⁵⁰ Davis and Shaw, 2001; Evans et al., 2016). Structured models that are built from long-term

51 demographic data collected from common garden experiments have emerged as powerful
52 technic to study the impact of climate change on species range shift (Merow et al., 2017;
53 Schwinnning et al., 2022). These structured models are increasingly utilized for several reasons.
54 First, structured models enable the manipulation of treatments that can isolate spatial and
55 temporal correlations between environmental factors, thus overcoming a main disadvantage
56 with many types of correlative studies (Leicht-Young et al., 2007). Second, structured models
57 link individual-level demographic trait to population demography allowing the investigation
58 of the demographic mechanisms behind vital rates (e.g. survival, fertility, growth and seed
59 germination) response environmental variation (Dahlgren et al., 2016; Louthan et al., 2022).
60 Third, these structured models can be used to identify which aspect of climate is more
61 important for population dynamics. For example, Life Table Response Experiment (LTRE)
62 build from structured models is an approach that has become widely used to understand
63 how a given treatment (eg. temperature or precipitation) could affect population dynamics
64 (Caswell, 1989; Iler et al., 2019; Morrison and Hik, 2007; O'Connell et al., 2024).

65 In this study, we used a mechanistic approach by combining geographically-distributed
66 field experiments, bayesian statistical modeling, and two-sex population projection modeling
67 to understand the demographic response of dioecious species to climate change and its
68 implications for future range dynamics. Our study system is a dioecious plant species (*Poa*
69 *arachnifera*) distributed along environmental gradients in the south-central US corresponding
70 to variation in temperature across latitude and precipitation across longitude. A previous
71 study on the same system showed that, despite a differentiation of climatic niche between
72 sexes, the female niche mattered the most in driving the environmental limits of population
73 viability (Miller and Compagnoni, 2022b). However that study did not use climate variables
74 preventing us from backcasting and forecasting the impact of climate change on dioecious
75 species. Here, we asked four questions:

- 76 1. What are the sex-specific vital rate responses to variation in temperature and precipitation
77 across the species' range ?
- 78 2. How sex-specific vital rates combine to determine the influence of climate variation on
79 population growth rate (λ) ?
- 80 3. What are the historical and projected changes in climate across the species range ?
- 81 4. What are the back-casted and fore-casted dynamics of this species' geographic niche
82 ($\lambda \geq 1$) and how does accounting for sex structure modify these predictions ?

⁸³ **Materials and methods**

⁸⁴ **Study species**

⁸⁵ Texas bluegrass (*Poa arachnifera*) is a dioecious perennial, summer-dormant cool-season (C3)
⁸⁶ grass that occurs in the south-central U.S. (Texas, Oklahoma, and southern Kansas) (Hitchcock,
⁸⁷ 1971). Average temperatures along the distribution of the species tend to decrease northward
⁸⁸ as a result of the influence of latitude: lower latitudes receive more heat from the sun over
⁸⁹ the course of a year. Similarly the average precipitation decrease eastward as a result of
⁹⁰ the influence of longitude: lower longitudes receive less precipitation over the year. Texas
⁹¹ bluegrass grows between October and May (growing season), with onset of dormancy often
⁹² from June to September (dormant season) (Kindiger, 2004). Flowering occurs in May and
⁹³ the species is wind pollinated (Hitchcock, 1971).

⁹⁴ **Common garden experiment**

⁹⁵ We set up a common garden experiment throughout and beyond the range of Texas bluegrass
⁹⁶ to enable study of sex-specific demographic responses to climate and the implications for range
⁹⁷ shifts. The novelty of this study lies in the fact that we use a precise climate variable to build
⁹⁸ a mechanistic model to forecast the response of species to climate change. Details of the exper-
⁹⁹ imental design are provided in Miller and Compagnoni (2022b); we provide a brief overview
¹⁰⁰ here. The common experiment was installed at 14 sites across a climatic gradient (Fig.1. At
¹⁰¹ each site, we established 14 blocks. For each block we planted three female and three male indi-
¹⁰² viduals that were clonally propagated from eight natural source populations of Texas bluegrass.
¹⁰³ The experiment was established in November 2013 and was census annually through 2016, pro-
¹⁰⁴ viding both spatial and inter-annual variation in climate. Each May (2014-2016), we collected
¹⁰⁵ individual demographic data including survival (alive or dead), growth (number of tillers),
¹⁰⁶ flowering status (reproductive or vegetative), and fertility (number of panicles, conditional on
¹⁰⁷ flowering). For the analyses that follow, we focus on the 2014-15 and 2015-16 transitions years.

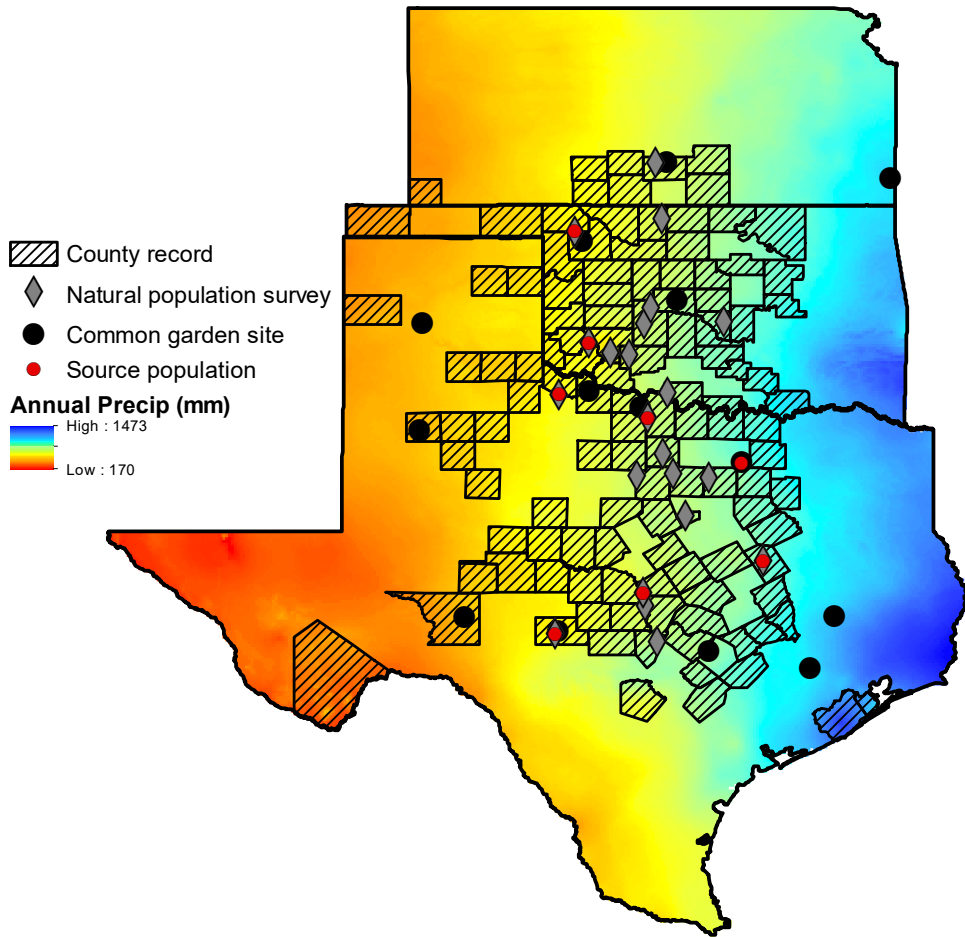


Figure 1: XXX

108 Climatic data collection

109 We downloaded monthly temperature and precipitation from Chelsa to describe observed
 110 climate conditions during our study period (Karger et al., 2017). These climate data were used
 111 as covariates in vital rate regressions, which allowed us to forecast and back-cast demographic
 112 responses to climate change based on observations across the common garden experiment.
 113 We aligned the climatic years to match demographic transition years (**May 1 – April 30**)¹
 114 rather than calendar years. Based on the natural history of this summer-dormant cool-season
 115 species, we divided each transition year into growing and dormant seasons. We define June
 116 through September as the dormant season and the rest of the year as the growing season.

¹I am not sure if these are actually the right dates.

117 Across years and sites, the experiment included substantial variation in growing and dormant
118 season temperature and precipitation (Fig. S-1, S-2).

119 To back-cast and forecast changes in climate, we downloaded projection data for
120 three 30-year periods: past (1901-1930), current (1990-2019) and future (2070-2100). Data
121 for these climatic periods were downloaded from four general circulation models (GCMs)
122 selected from the Coupled Model Intercomparison Project Phase 5 (CMIP5). The GCMs
123 are MIROC5, Australian Community Climate and Earth System Simulator (ACCESS1-3),
124 CESM1-BGC, Centro Euro-Mediterraneo per I Cambiamenti Climatici (CMCC-CM) and
125 were downloaded from chelsa (Sanderson et al., 2015). We evaluated future climate
126 projections from two scenarios of representative concentration pathways (RCPs): RCP4.5, an
127 intermediate-to-pessimistic scenario assuming a radiative forcing to amount to 4.5 Wm^{-2} by
128 2100, and RCP8.5, a pessimistic emission scenario which project a radiative forcing to amount
129 to 8.5 Wm^{-2} by 2100 (Schwalm et al., 2020; Thomson et al., 2011).

130 Sex ratio experiment

131 We conducted a sex-ratio experiment on a site close (1 km) to a natural population of the
132 focal species at the center of the range to estimate the effect of sex-ratio variation on female
133 reproductive success. Details of the experiment are provided in Compagnoni et al. (2017) and
134 Miller and Compagnoni (2022b). In short, we established 124 experimental populations on
135 plots measuring $0.4 \times 0.4\text{m}$ and separated by at least 15m from each other at that site. We chose
136 15m because our pilot data show that more than 90% of wind pollination occurred within 13m.
137 We varied population density (1-48 plants/plot) and sex ratio (0%-100% female) across the ex-
138 perimental populations, and we replicated 34 combinations of density-sex ratios. We collected
139 the number of panicles from a subset of females in each plot and collected the number of
140 seeds in each panicle. Since the number of panicles (proxy of reproduction effort) does not nec-
141 essarily reflect reproduction success in *Poar arachnifera*, we accessed reproduction success (seed
142 fertilized) using greenhouse-based germination and trazolium-based seed viability assays.

143 We used the sex-ratio to estimate the probability of viability and the germination rate.
144 Seed viability was modeled with a binomial distribution where the probability of viability
145 (v) was given by:

$$146 \quad v = v_0 * (1 - OSR^\alpha) \quad (1)$$

147 where OSR is the operational sex ratio (proportion of panicles that were female) in the
148 experimental populations. The properties of the above function is supported by our previous
149 work (Compagnoni et al., 2017). Here, seed viability is maximized at v_0 as OSR approaches

150 zero (strongly male-biased) and goes to zero as *OSR* approaches 1 (strongly female-biased).
151 Parameter α controls how viability declines with increasing female bias.

152 We used a binomial distribution to model the germination data from greenhouse trials.
153 Given that germination was conditional on seed viability, the probability of success was given
154 by the product $v*g$, where v is a function of *OSR* (Eq. 1) and g is assumed to be constant.

155 Sex specific demographic responses to climate

156 We used individual level measurements of survival, growth (number of tillers), flowering, num-
157 ber of panicles to independently develop Bayesian mixed effect models describing how each
158 vital rate varies as a function of sex, size, precipitation of growing and dormant season and tem-
159 perature of of growing and dormant season. We fit vital rate models with second-degree poly-
160 nomial functions for the influence of climate. We included a second-degree polynomial because
161 we expected that climate variables would affect vital rates through a hump-shaped relationship.

162 We centered and standardized all climatic predictors to facilitate model convergence.
163 However, Size was on a natural logarithm scale. We included site,source, and block as
164 random effect. All the vital rate models used the same linear and quadratic predictor for
165 the expected value (μ) (Eq.2) . However, we applied a different link function ($f(\mu)$) depending
166 on the distribution the vital rate. We modeled survival and flowering data with a Bernoulli
167 distribution. We modeled the growth (tiller number) with a zero-truncated Poisson inverse
168 Gaussian distribution. Fertility (panicle count) was model as zero-truncated negative binomial.

$$f(\mu) = \beta_0 + \beta_1 \text{size} + \beta_2 \text{sex} + \beta_3 \text{pptgrow} + \beta_4 \text{pptdorm} + \beta_5 \text{tempgrow} + \beta_6 \text{tempdorm} \\ + \beta_7 \text{pptgrow*sex} + \beta_8 \text{pptdorm*sex} + \beta_9 \text{tempgrow*sex} + \beta_{10} \text{tempdorm*sex} \\ + \beta_{11} \text{size*sex} + \beta_{12} \text{pptgrow*tempgrow} + \beta_{13} \text{pptdorm*tempdorm} \quad (2) \\ + \beta_{14} \text{pptgrow*tempgrow*sex} + \beta_{15} \text{pptdorm*tempdorm*sex} + \beta_{16} \text{pptgrow}^2 \\ + \beta_{17} \text{pptdorm}^2 + \beta_{18} \text{tempgrow}^2 + \beta_{19} \text{tempdorm}^2 + \beta_{20} \text{pptgrow}^2 * \text{sex} \\ + \beta_{21} \text{pptdorm}^2 * \text{sex} + \beta_{22} \text{tempgrow}^2 * \text{sex} + \beta_{23} \text{tempdorm}^2 * \text{sex} + \phi + \rho + \nu$$

170 where β_0 is the grand mean intercept, β_1 is the size dependent slopes. *size* was on a natural log-
171 arithm scale. $\beta_2 \dots \beta_{13}$ represent the climate dependent slopes. $\beta_{14} \dots \beta_{23}$ represent the sex-climate
172 interaction slopes. *pptgrow* is the precipitation of the growing season (standardized to mean
173 zero and unit variance), *tempgrow* is the temperature of the growing season (standardized to
174 mean zero and unit variance), *pptdorm* is the precipitation of the dormant season (standardized
175 to mean zero and unit variance), *tempdorm* is the temperature of the dormant season (standard-
176 ized to mean zero and unit variance). The model also includes normally distributed random

177 effects for block-to-block variation ($\phi \sim N(0, \sigma_{block})$) and source-to-source variation that is
 178 related to the provenence of the seeds used to establish the common garden ($\rho \sim N(0, \sigma_{source})$),
 179 site to site variation ($\nu \sim N(0, \sigma_{site})$). We fit survival, growth, flowering models with generic
 180 weakly informative priors for coefficients ($\mu = 0, \sigma = 1.5$) and variances ($\gamma[0.1, 0.1]$). **We fit**
 181 **fertility model with regularizing priors for coefficients ($\mu=0, \sigma=0.15$)**. We ran three chains
 182 for 1000 samples for warmup and 4000 for interactions, with a thinning rate of 3. We accessed
 183 the quality of the models using trace plots and predictive check graphs (Piironen and Vehtari,
 184 2017) (Fig. S-4). To understand the effect of climate on vital rates, we got the 95 % credible
 185 interval of the posterior distribution. Then we assumed that there is 95 % probability that the
 186 true (unknown) estimates would lie within that interval, given the evidence provided by the
 187 observed data for each vital rate. All models were fit in Stan (Stan Development Team, 2023).

188 Influence of climate variation on population growth rate

189 To understand the effect of climate on population growth rate, we used the vital rate estimated
 190 earlier to build a matrix projection model (MPM) structured by size (number of tillers),
 191 sex and climate (dormant and growing) as covariate. Let $F_{x,z,t}$ and $M_{x,z,t}$ be the number of
 192 female and male plants of size x in year t present at a location that has z as climate, where
 193 $x \in \{1, 2, \dots, U\}$ and U is the maximum number of tillers a plant can reach (here 95th percentile
 194 of observed maximum size). Let F_t^R and M_t^R be the new recruits, which we assume do not
 195 reproduce in their first year. We assume that the parameters of sex ratio-dependent mating
 196 (Eq. 1) do not vary with climate. For a pre-breeding census, the expected numbers of recruits
 197 in year $t+1$ is given by:

$$198 F_{t+1}^R = \sum_{x=1}^U [p^F(x,z) \cdot c^F(x,z) \cdot d \cdot v(\mathbf{F}_t, \mathbf{M}_t) \cdot m \cdot \rho] F_{x,z,t} \quad (3)$$

$$199 M_{t+1}^R = \sum_{x=1}^U [p^F(x,z) \cdot c^F(x,z) \cdot d \cdot v(\mathbf{F}_t, \mathbf{M}_t) \cdot m \cdot (1-\rho)] F_{x,z,t} \quad (4)$$

200 where p^F and c^F are flowering probability and panicle production for females of size x , d
 201 is the number of seeds per female panicle, v is the probability that a seed is fertilized, m is
 202 the probability that a fertilized seed germinates, and ρ is the primary sex ratio (proportion
 203 of recruits that are female), z is the climate. Seed fertilization depends on the OSR of panicles
 204 (following Eq. 1) which was derived from the $U \times 1$ vectors of population structure \mathbf{F}_t and \mathbf{M}_t :

$$205 v(\mathbf{F}_t, \mathbf{M}_t) = v_0 * \left[1 - \left(\frac{\sum_{x=1}^U p^F(x,z) c^F(x,z) F_{x,z,t}}{\sum_{x=1}^U p^F(x,z) c^F(x,z) F_{x,z,t} + p^M(x,z) c^M(x,z) M_{x,z,t}} \right)^\alpha \right] \quad (5)$$

206 Thus, the dynamics of the size-structured component of the population are given by:

207

$$F_{y,t+1} = [\sigma \cdot g^F(y, x=1, z)] F_t^R + \sum_{x=1}^U [s^F(x, z) \cdot g^F(y, x, z)] F_{x,z,t} \quad (6)$$

208

$$M_{y,t+1} = [\sigma \cdot g^M(y, x=1, z)] M_t^R + \sum_{x=1}^U [s^M(x, z) \cdot g^M(y, x, z)] M_{x,z,t} \quad (7)$$

209 In the two formula above, the first term indicates seedlings that survived their first year and en-
210 ter the size distribution of established plants. Instead of using *P. arachnifera* survival probability,
211 we used the seedling survival probability (σ) from demographic studies of the hermaphroditic
212 congener *Poa autumnalis* in east Texas (T.E.X. Miller and J.A. Rudgers, *unpublished data*), and we
213 assume this probability was constant across sexes and climatic variables. We did this because
214 we had little information on the early life cycle transitions of greenhouse-raised transplants.
215 We also assume that $g(y, x=1)$ is the probability that a surviving seedlings reach size y ,
216 the expected future size of 1-tiller plants from the transplant experiment. The second term
217 represents survival and size transition of established plants from the previous year, where
218 s and g give the probabilities of surviving at size x and growing from sizes x to y , respectively,
219 and superscripts indicate that these functions may be unique to females (F) and males (M).

220 Since the two-sex MPM is nonlinear (vital rates affect and are affected by population
221 structure) we estimated the asymptotic geometric growth rate (λ) by numerical simulation,
222 and repeated this across a range of climate.

223 Identifying the mechanisms of population growth rate sensitivity to climate

224 To identify which aspect of climate is most important for population viability, we used
225 a "random design" Life Table Response Experiment (LTRE). We used the RandomForest
226 package to fit a regression model with θ as predictors and λ as response (Ellner et al., 2016;
227 Liaw et al., 2002). The LTRE approximates the variation in λ in response to climate covariates
228 and their interaction (Caswell, 2000; Hernández et al., 2023):

229

$$Var(\lambda_c) \approx \sum_{i=-1}^n \sum_{j=1}^n Cov(\theta_i, \theta_j, \theta_{ij}) + Var(\epsilon) \quad (8)$$

230 where, θ_i , θ_j , θ_{ij} represent respectively the fitted regression slope for the covariates of the
231 dormant season, j the covariates of the growing season and ij the covariates of their interactions.

232 To identify the mechanism by which climate affects population growth rate for each sex,
233 we decomposed the effect of each climate variable (here Climate) on population growth rate (λ)
234 into contribution arising from the effect on each stage-specific vital rate (Caswell, 2000). At this

235 end we used another LTRE with a "regression design". The LTRE with a "regression design" ap-
236 proximates the change in λ with climate as the product of the sensitivity of λ to the parameters
237 times the sensitivity of the parameters to climate, summed over all parameters (Caswell, 1989):

$$238 \quad \frac{\partial \lambda}{\partial \text{climate}} \approx \sum_i \frac{\partial \lambda}{\partial \theta_i^F} \frac{\partial \theta_i^F}{\partial \text{climate}} + \frac{\partial \lambda}{\partial \theta_i^M} \frac{\partial \theta_i^M}{\partial \text{climate}} \quad (9)$$

239 where, θ_i^F and θ_i^M represent sex-specific parameters: the regression coefficients for the
240 intercepts and slopes of size-dependent vital rate functions. Because LTRE contributions are
241 additive, we summed across vital rates to compare the total contributions of female and male
242 parameters.

243 Impact of climate change on niche and range shifts

244 A species' ecological niche can be defined as the range of resources and conditions (physical
245 and environmental) allowing the species to maintain a viable population ($\lambda > 1$) (Hutchinson
246 et al., 1978; Maguire Jr, 1973). To understand the impact of climate change on species niche
247 shifts, we estimated the probability of population viability being greater than 1, $\text{Pr}(\lambda > 1)$ conditional to two environmental axes: (i) temperature and precipitation of the dormant season
248 and (ii) temperature and precipitation of the growing season. $\text{Pr}(\lambda > 1)$ was calculated using
249 the proportion of the Markov chain Monte Carlo iterations that lead to a $\lambda > 1$ (Diez et al., 2014).
250 $\text{Pr}(\lambda > 1)$ was mapped onto geographic layers of three state (Texas, Oklahoma and Kansas) to
251 delineate past, current and future potential distribution of the species. To do so, we estimated
252 $\text{Pr}(\lambda > 1)$ conditional to all climate covariates for each pixel (1km*1km) across the species range.
253 Because of amount of the computation involve in the Markov chain Monte Carlo iterations,
254 use only 100 posterior samples to estimate $\text{Pr}(\lambda > 1)$ across the Texas, Oklahoma and Kansas.

256 All calculations were processed in parallel using open-source software on the Rice
257 Super computer (NOTS) and the German Centre for Integrative Biodiversity Research (iDiv)
258 High-Performance Computing (HPC) Cluster.

259 Results

260 Sex specific demographic response to climate change

261 Most vital rates were strongly climate dependent, but the magnitude of their response differed
262 between sexes suggesting a sex-specific demographic response to climate. Survival and flower-
263 ing were strongly more dependent on climate than growth (number of tillers) and reproduction

(number of panicles) (Fig.S-5; Fig. S-6). In addition, we found opposite patterns in the direction of the effect on seasonal climate on the probability of survival and flowering. The growing season (precipitation) has a negative effect on the probability of survival, number of tillers, and the probability of flowering, whereas the dormant season has a positive effect on these vital rates. Unlike precipitation, temperature had different effects on different vital rates. Temperature of the growing season has a positive effect of the probability of survival, a negative effect of the probability of flowering, and the number of tillers, but no significant effect on the number of panicles. Further, there was a female survival and flowering advantage across both climatic seasons (Figures. 3A-3D, 3I-3L). On the contrary, there was a male panicle advantage across all climatic variables (Figure3M-3P). Counter-intuitively, there was no significant sex growth advantage in all season climatic variables (Figures. 3E-3H). Plant size and sex interaction was significant for all vitals rates (Fig. S-6). For survival, flowering and reproduction the interaction between temperature and precipitation of the growing season and dormant season was not significant (Fig. S-6). However, for growth the interaction between temperature and precipitation of the growing season and dormant season was significantly higher than zero (Fig. S-6).

Climate change alter population viability

We estimated the predicted response of population growth rate (population fitness) to seasonal climate gradients using two models: one accounting for one sex (female dominant) and another one accounting for two sexes. Consistent with the effect of climate on the individual vital rate, we found a strong effect of seasonal climate on population fitness (Fig.2). For both models (female dominant and two sexes), population fitness decreased with an increase of precipitation of growing season(Fig.2 A, C). In contrast population fitness increased with precipitation of the dormant season. Furthermore, population fitness was maximized between 14 and 17 °C and decreases to zero just beyond 32 °C during the growing season (Fig.2 B). Similarly population fitness was maximized between 27 and 31 °C and decreases to zero just beyond 20 °C during the growing season (Fig.2 D). We have also detected a strong effect of the past and future climate on population growth rate. However, the magnitude of the effect of future climate on population growth rate was different between gas-scenario emissions. Under past climate conditions, population growth rate decreased below one for temperature of the growing season. A moderate emission gas scenario (RCP4.5) has a no effect on the population growth rate while a high emission scenario (RCP8.5) has a strong negative effect on population growth rate (Fig.2 B, D).

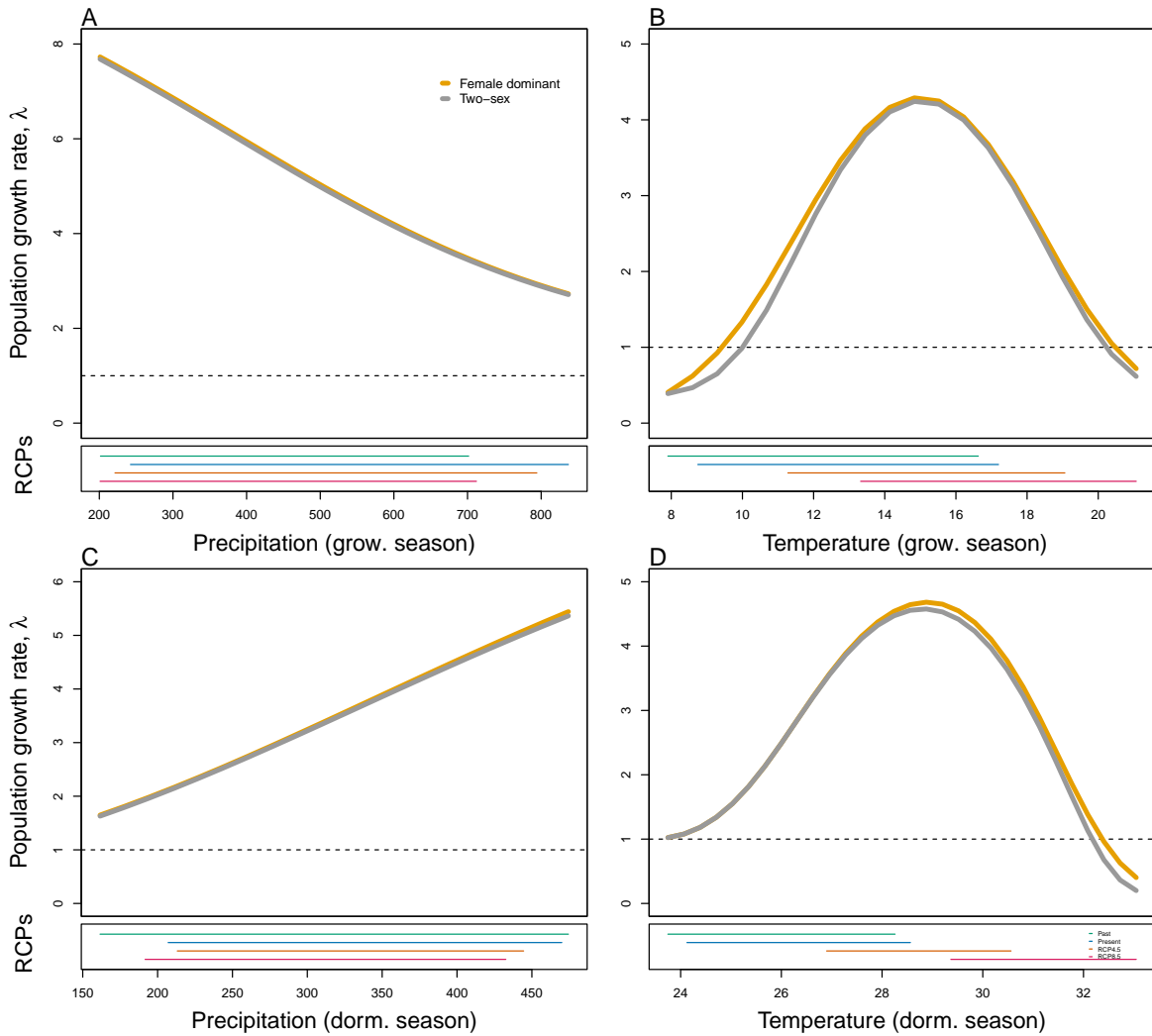


Figure 2: Population growth rate (λ) as a function of Precipitation of the growing season (A), Temperature of the growing season (B), Precipitation of the dormant season (C), Temperature of the dormant season (D). The grey curve shows prediction by the two-sex matrix projection model that incorporates sex-specific demographic responses to climate with sex ratio dependent seed fertilization. The orange curve represents the prediction by the female dominant matrix projection model. The dashed horizontal line indicates the limit of population viability ($\lambda = 1$). Lower panels below each data panel show climate values (past climate, present and future climates). For future climate, we show a Representation Concentration Pathways (RCP) 4.5 and 8.5. Values of (λ) are derived from the mean climate variables across 4 GCMs (MIROC5, ACCESS, CCMC, CES)

296 Temperature as a driver of population viability decline

297 Population viability was most sensitive to change in temperature of the growing season and
 298 temperature of the dormant season (Supporting Information S-7). LTRE decomposition reveals
 299 that, for each sex, the reduction of lambda for high value of temperature of the growing
 300 season was driven by a reduction of survival rate, growth rate, flowering and a reduction in

301 number of panicles(Fig.3 A, B). However, the reduction of population growth rate for higher
 302 value of temperature of the dormant season was driven by only the female (Fig.3 C, D).

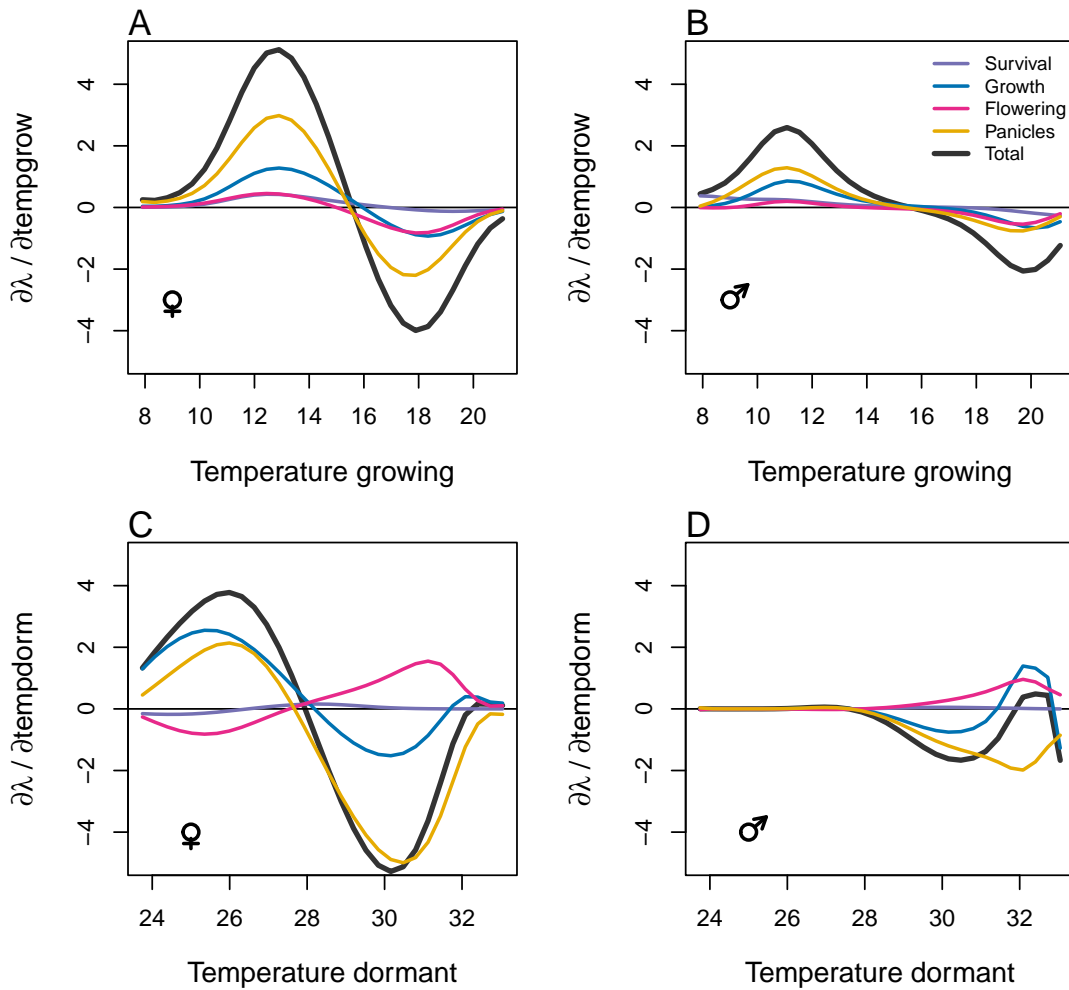


Figure 3: Life table response experiment decomposition of the sensitivity of (λ) to temperature of growing season (A,B) and dormant season (C,D) into additive vital rate contributions of males females based on posterior mean parameter estimates.

303 Climatic change induce niche and range shifts

304 Our results suggest niche sifts for both dormant and growing season (Fig. 4). However, the
 305 model that does not account for sex structure overestimate the magnitude of niche shifts (Fig.
 306 4 D). Our demographically based range predictions broadly captured the known distribution

of the species . More specifically, the predicted population viable ($\lambda > 1$) matches the presence and absence of the species (Fig. 5 B, Fig. 6 B). Furthermore, viable populations of *P. arichnifera* were only predicted at the center of the range for current climatic conditions (Fig. 5 B). Although *P. arichnifera* was predicted to have suitable habitat in the center of the range under the current climate, global warming (regardless of the future scenario of carbon emission used) is predicted to reduce much of the suitable habitat (Fig. 5 C, D). Most of the suitable habitat will move toward the North at range edge. In contrast, suitability increase across the range under RCP 4.5 which is the scenario assuming moderate carbon emission by 2100.

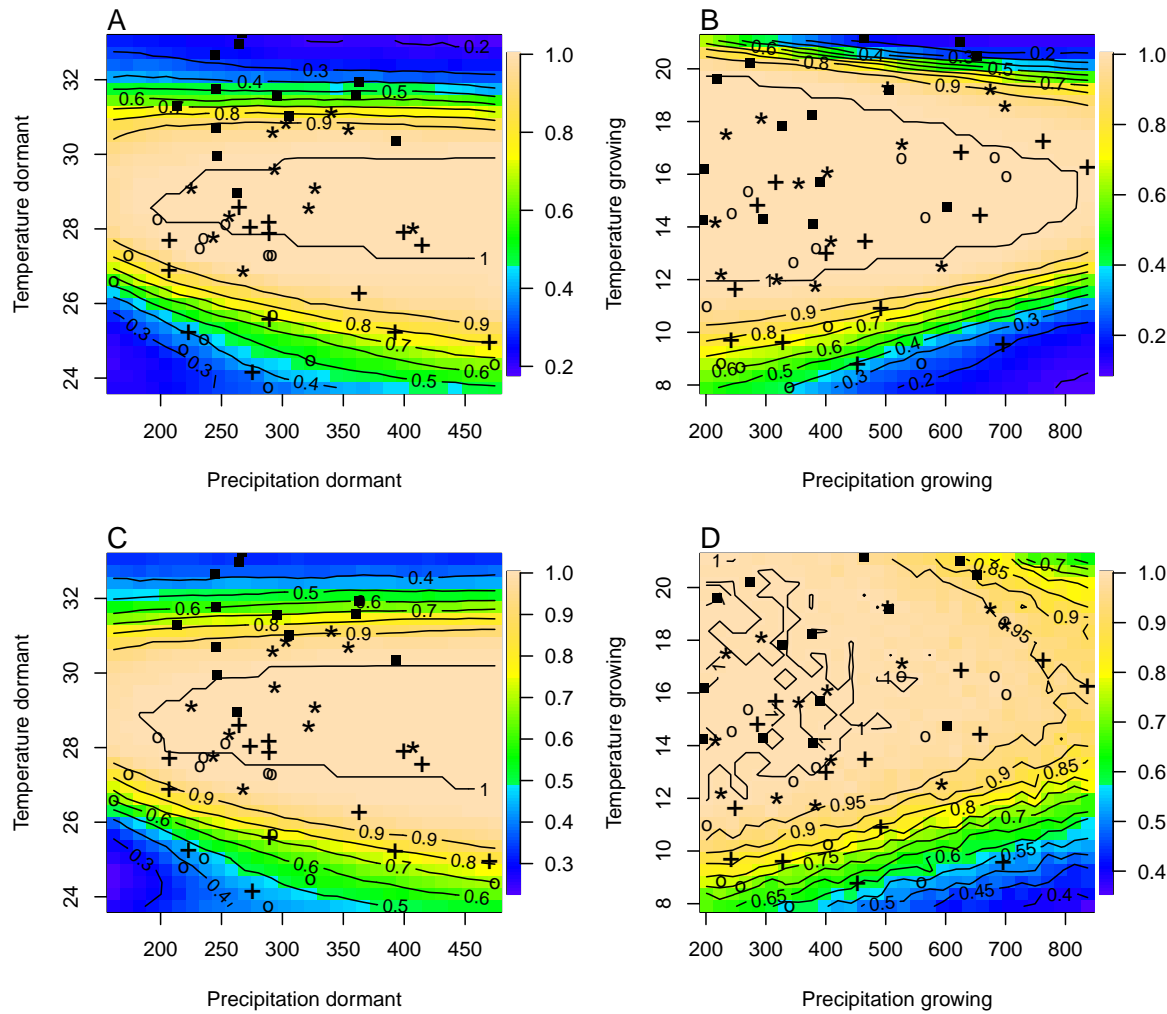


Figure 4: A two-dimensional representation of the predicted niche shift over time (past, present and future climate conditions) based on $\text{Pr}(\lambda > 1)$. Contours show predicted probabilities of self-sustaining populations $\text{Pr}(\lambda > 1)$ conditional on precipitation and temperature of the dormant and growing season. (A) Niche of dormant season for the two sex model , (B) Niche of growing season for the two sex model, Niche of dormant season for female dominant model (C), Niche of growing season for female dominant model. "o" Past, "+" Current,"*" RCP 4.5, "■" RCP 8.5

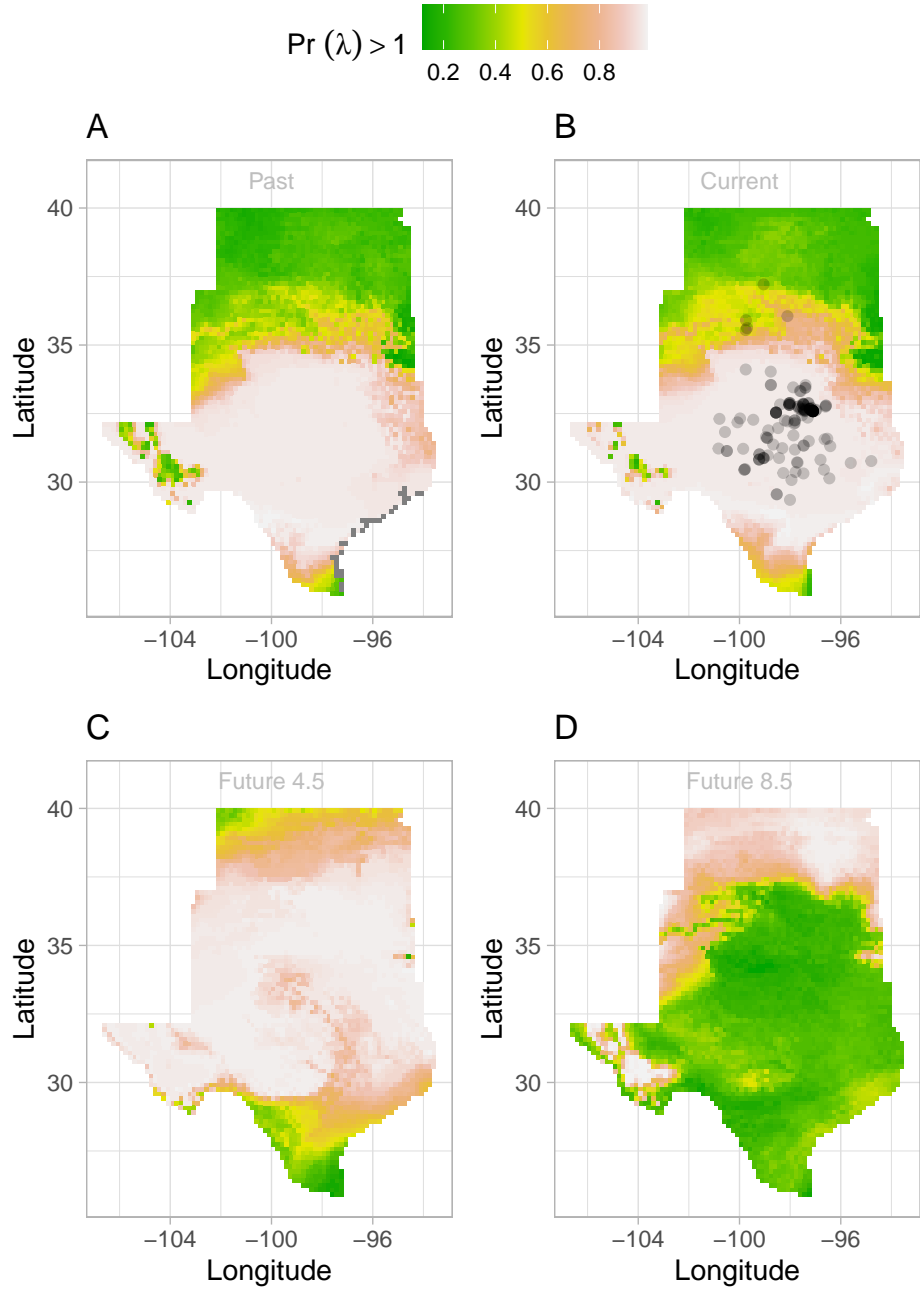


Figure 5: (A) Past ,(B) Current , Future (2070–20100) (C and D) predicted range shift based on population growth rate using the two sex model. Future projections were based on CMC. The black circles on panel B indicate all known presence points collected from GBIF from 1990 to 2019, which corresponds to the current condition in our prediction. The occurrences of GBIFs are distributed inwith higher population fitness habitat ($\lambda > 1$) , confirming that our study approach can reasonably predict range shifts.

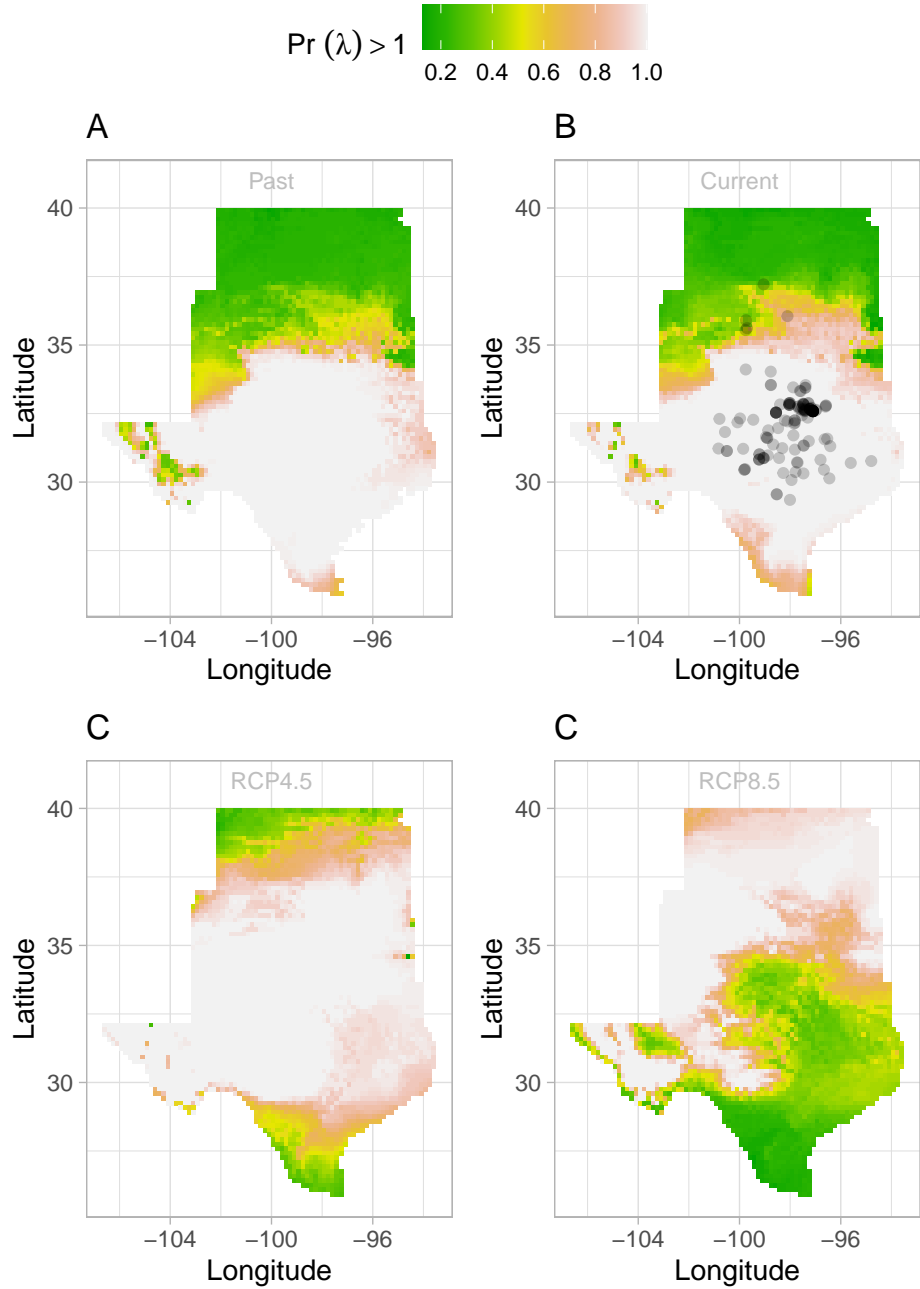


Figure 6: Past (A), Current (B), Future (2070–20100) (C and D) predicted range shift based on population growth rate using the female dominant model. Future projections were based on the average population growth rate CES. The black circles on panel B indicate all known presence points collected from GBIF from 1990 to 2019, which corresponds to the current condition in our prediction. The occurrences of GBIFs are distributed in with higher population fitness habitat ($\lambda > 1$), confirming that our study approach can reasonably predict range shifts.

315 **Discussion**

316 We forecasted range shifts in dioecious species using climate-demographic models. Three
317 general patterns emerged from our analysis. First, our Bayesian mixed effect model predicts
318 that seasonal climate (temperature and precipitation) affects sex-demographic processes in
319 distinctive and contrasting ways. While climate has a significant effect on the probability of
320 survival and growth, it has no effect on the number of panicles. Second, future climate, by
321 increasing seasonal temperature, will lead to decline in population viability and favor range
322 shifts. Third, using only one sex to forecast range shifts of dioecious under climate change
323 could lead to an underestimation of the impact of climate change on species.

324 Our results indicate a sex-specific demographic response to climate change. Females have
325 higher survival rate and fertility rate than males. This result is not unique to our study system
326 and has been observed in a range of abiotic pollen dispersal species across climatic gradients
327 (Sasaki et al., 2019; Welbergen et al., 2008; Zhao et al., 2012). Several hypotheses could explain
328 the observed demographic advantage of females over males for survival and flowering and
329 the opposite for growth and number of panicles. The trade-off between fitness traits (survival,
330 growth fertility) due to resource limitation and the pollination mode of our study species (wind
331 pollinated) could explain such a result (Cipollini and Whigham, 1994; Freeman et al., 1976).
332 For most species, females often pay more for reproduction than males due to the requirement
333 to develop seeds and fruits (Hultine et al., 2016). However, several studies reported a higher
334 cost of reproduction for males in wind pollinated species due to the larger amounts of pollen
335 they produce (Bruijning et al., 2017; Bürl et al., 2022; Cipollini and Whigham, 1994; Field et al.,
336 2013). In addition to life history trade-off, other among site difference in non-climatic factors
337 such as soil, or biotic interactions could explain decline in vital rate as an indirect effects of
338 increase in temperature (Alexander et al., 2015; Schultz et al., 2022).

339 Under current conditions, most populations across the range are viable. This result
340 could be explained by two hypotheses. First, demographic compensation whereby an
341 increase of one vital rate is coupled with a decrease of another vital rate could explain viable
342 populations in harsh conditions at the range edge (Doak and Morris, 2010; Nomoto and
343 Alexander, 2021; Villegas et al., 2015). In our system, a decrease in fertility and survival rate
344 was counterbalanced by an increase in flowering rate, preventing the population growth
345 rate from declining even at range edge during the dormant season. Second, local adaptation
346 at the edge of the range could explain the viable population throughout the range (Miller
347 and Compagnoni, 2022b). Our study was based on a common garden experiment; therefore,
348 individuals planted in climatic conditions that are similar to their source populations climatic
349 conditions were less impacted by stressful environmental conditions. One important question

350 to ask is: what is the role of local adaptation in buffering species response to climate change.
351 Adding another predictor to our complex model would have lead to overfitting. Therefore,
352 our model does not shed light on the importance of local adaptation in species response to
353 climate change. The role of local adaptation in mitigating population response to climate
354 should be the next step in forecasting species response to climate.

355 Our LTRE analysis reveals that a small changes in temperature of the growing and
356 dormant season could have a larger impact on population viability. Temperature can impact
357 plant populations through different mechanisms. Increasing temperature could increase
358 evaporative demand, affect plant phenology (Iler et al., 2019; McLean et al., 2016; Sherry et al.,
359 2007), and germination rate (Reed et al., 2021). The potential for temperature to influence
360 these different processes changes seasonally (Konapala et al., 2020). For example, studies
361 suggested that species that are active during the growing season such as cool grass species
362 can have delayed phenology in response to global warming, particularly if temperatures rise
363 above their physiological tolerances (Cleland et al., 2007; Williams et al., 2015). In addition,
364 high temperature during the growing season by affecting pollen viability, fertilization could
365 affect seed formation and germination (Hatfield and Prueger, 2015; Sletvold and Ågren, 2015).
366 Temperature could also affected OSR. That variation in OSR could affect population growth
367 rate by altering females' fitness (Knight et al., 2005; Petry et al., 2016).

368 We found evidence of climatic niche shifts for the models account for sex structure
369 and for the model that does not account for sex structure. However the model that does
370 not account for sex structure overestimated species niche, suggesting that using one sex to
371 predict niche shifts could be misleading. Climatic conditions that are not optimal under
372 current conditions will be optimal for the species over the next years particularly at the edge
373 of species. Pollen dispersal may allow plants to resist faster climate change because pollen
374 dispersal may provide the local genetic diversity necessary to adapt at the leading edge of the
375 population (Corlett and Westcott, 2013; Duputié et al., 2012; Kremer et al., 2012). Since wind
376 pollination is most effective at short distances, it is most often found in plant species growing
377 at high density such as our study species, dispersal limitation or interspecific interaction
378 might constrain the species to a narrower realized niche (Aguilée et al., 2016; Pulliam, 2000).

379 Our result suggest that climate change will drive range shifts and the magnitude and rate
380 of that range shift could be underestimated when tracking only one sex (Fig. S-9, Fig. S-10, Fig.
381 S-11, Fig. S-12, Fig. S-13, Fig. S-14). Since a small change in both sexes affect population viability,
382 OSR change due to climate change in *P. arachnifera* could induce range shifts. In *V. edulis*
383 increase in male frequency induce range shifts by reducing pollen limitation in conditions
384 that were not suitable (Petry et al., 2016). Three years represent a relatively decent time
385 for demographic study for common garden experiments across climatic gradient. Thus our

386 models can only capture a certain range of demographic and environmental variability (Fig.
387 S-8). Moreover, our future projections require extrapolation to warmer or colder conditions
388 than observed in our experiment and subsequently should be interpreted with caution.
389 Despite all these limitations, the qualitative implications of a negative response of species
390 to increase temperature (dormant and growing season) seems consistent across all climate
391 all GCMs (Fig. S-9, Fig. S-10, Fig. S-11, Fig. S-12, Fig. S-13, Fig. S-14). Most of the suitable
392 areas move toward the North in response to climate change. Climate change will affect
393 population growth rate primarily through the response of female which is more sensitive
394 to climate change. Our work suggest that current climate may not affect population viability,
395 but populations may be impacted negatively over the next decades in response to a climate
396 change. This is key because most conservation actions are design from data on current
397 responses to climate, rather than future response to climate (Sletvold et al., 2013).

398 Conclusion

399 Acknowledgements

400 This research was supported by XXXX.

401 Authorship statement

402 All authors discussed all aspects of the research and contributed to developing methods,
403 analyzing data, and writing and revising the paper.

404 Conflict of interest statement

405 The authors have none to declare.

406 **References**

- 407 Aguilée, R., Raoul, G., Rousset, F., and Ronce, O. (2016). Pollen dispersal slows geographical
408 range shift and accelerates ecological niche shift under climate change. *Proceedings of the
409 National Academy of Sciences*, 113(39):E5741–E5748.
- 410 Alexander, J. M., Diez, J. M., and Levine, J. M. (2015). Novel competitors shape species'
411 responses to climate change. *Nature*, 525(7570):515–518.
- 412 Bertrand, R., Lenoir, J., Piedallu, C., Riofrío-Dillon, G., De Ruffray, P., Vidal, C., Pierrat, J.-C.,
413 and Gégout, J.-C. (2011). Changes in plant community composition lag behind climate
414 warming in lowland forests. *Nature*, 479(7374):517–520.
- 415 Bruijning, M., Visser, M. D., Muller-Landau, H. C., Wright, S. J., Comita, L. S., Hubbell, S. P.,
416 de Kroon, H., and Jongejans, E. (2017). Surviving in a cosexual world: A cost-benefit
417 analysis of dioecy in tropical trees. *The American Naturalist*, 189(3):297–314.
- 418 Bürli, S., Pannell, J. R., and Tonnabel, J. (2022). Environmental variation in sex ratios and
419 sexual dimorphism in three wind-pollinated dioecious plant species. *Oikos*, 2022(6):e08651.
- 420 Caswell, H. (1989). Analysis of life table response experiments i. decomposition of effects
421 on population growth rate. *Ecological Modelling*, 46(3-4):221–237.
- 422 Caswell, H. (2000). *Matrix population models*, volume 1. Sinauer Sunderland, MA.
- 423 Cipollini, M. L. and Whigham, D. F. (1994). Sexual dimorphism and cost of reproduction
424 in the dioecious shrub *lindera benzoin* (lauraceae). *American Journal of Botany*, 81(1):65–75.
- 425 Cleland, E. E., Chuine, I., Menzel, A., Mooney, H. A., and Schwartz, M. D. (2007). Shifting
426 plant phenology in response to global change. *Trends in ecology & evolution*, 22(7):357–365.
- 427 Compagnoni, A., Steigman, K., and Miller, T. E. (2017). Can't live with them, can't live
428 without them? balancing mating and competition in two-sex populations. *Proceedings of
429 the Royal Society B: Biological Sciences*, 284(1865):20171999.
- 430 Corlett, R. T. and Westcott, D. A. (2013). Will plant movements keep up with climate change?
431 *Trends in ecology & evolution*, 28(8):482–488.
- 432 Czachura, K. and Miller, T. E. (2020). Demographic back-casting reveals that subtle
433 dimensions of climate change have strong effects on population viability. *Journal of Ecology*,
434 108(6):2557–2570.

- 435 Dahlgren, J. P., Bengtsson, K., and Ehrlén, J. (2016). The demography of climate-driven and
436 density-regulated population dynamics in a perennial plant. *Ecology*, 97(4):899–907.
- 437 Davis, M. B. and Shaw, R. G. (2001). Range shifts and adaptive responses to quaternary
438 climate change. *Science*, 292(5517):673–679.
- 439 Diez, J. M., Giladi, I., Warren, R., and Pulliam, H. R. (2014). Probabilistic and spatially variable
440 niches inferred from demography. *Journal of ecology*, 102(2):544–554.
- 441 Doak, D. F. and Morris, W. F. (2010). Demographic compensation and tipping points in
442 climate-induced range shifts. *Nature*, 467(7318):959–962.
- 443 Duputié, A., Massol, F., Chuine, I., Kirkpatrick, M., and Ronce, O. (2012). How do genetic cor-
444 relations affect species range shifts in a changing environment? *Ecology letters*, 15(3):251–259.
- 445 Eberhart-Phillips, L. J., Küpper, C., Miller, T. E., Cruz-López, M., Maher, K. H., Dos Remedios,
446 N., Stoffel, M. A., Hoffman, J. I., Krüger, O., and Székely, T. (2017). Sex-specific early
447 survival drives adult sex ratio bias in snowy plovers and impacts mating system and
448 population growth. *Proceedings of the National Academy of Sciences*, 114(27):E5474–E5481.
- 449 Ellis, R. P., Davison, W., Queirós, A. M., Kroeker, K. J., Calosi, P., Dupont, S., Spicer, J. I.,
450 Wilson, R. W., Widdicombe, S., and Urbina, M. A. (2017). Does sex really matter? explaining
451 intraspecies variation in ocean acidification responses. *Biology letters*, 13(2):20160761.
- 452 Ellner, S. P., Childs, D. Z., Rees, M., et al. (2016). Data-driven modelling of structured
453 populations. *A practical guide to the Integral Projection Model*. Cham: Springer.
- 454 Evans, M. E., Merow, C., Record, S., McMahon, S. M., and Enquist, B. J. (2016). Towards
455 process-based range modeling of many species. *Trends in Ecology & Evolution*, 31(11):860–871.
- 456 Field, D. L., Pickup, M., and Barrett, S. C. (2013). Comparative analyses of sex-ratio variation
457 in dioecious flowering plants. *Evolution*, 67(3):661–672.
- 458 Freeman, D. C., Klikoff, L. G., and Harper, K. T. (1976). Differential resource utilization by
459 the sexes of dioecious plants. *Science*, 193(4253):597–599.
- 460 Gamelon, M., Grøtan, V., Nilsson, A. L., Engen, S., Hurrell, J. W., Jerstad, K., Phillips, A. S.,
461 Røstad, O. W., Slagsvold, T., Walseng, B., et al. (2017). Interactions between demography
462 and environmental effects are important determinants of population dynamics. *Science
Advances*, 3(2):e1602298.

- ⁴⁶⁴ Gissi, E., Schiebinger, L., Hadly, E. A., Crowder, L. B., Santoleri, R., and Micheli, F. (2023).
⁴⁶⁵ Exploring climate-induced sex-based differences in aquatic and terrestrial ecosystems to
⁴⁶⁶ mitigate biodiversity loss. *nature communications*, 14(1):4787.
- ⁴⁶⁷ Hatfield, J. and Prueger, J. (2015). Temperature extremes: effect on plant growth and
⁴⁶⁸ development. *weather clim extrem* 10: 4–10.
- ⁴⁶⁹ Hernández, C. M., Ellner, S. P., Adler, P. B., Hooker, G., and Snyder, R. E. (2023). An exact
⁴⁷⁰ version of life table response experiment analysis, and the r package exactltre. *Methods*
⁴⁷¹ in *Ecology and Evolution*, 14(3):939–951.
- ⁴⁷² Hitchcock, A. S. (1971). *Manual of the grasses of the United States*, volume 2. Courier Corporation.
- ⁴⁷³ Hultine, K. R., Grady, K. C., Wood, T. E., Shuster, S. M., Stella, J. C., and Whitham, T. G. (2016).
⁴⁷⁴ Climate change perils for dioecious plant species. *Nature Plants*, 2(8):1–8.
- ⁴⁷⁵ Hutchinson, G. E. et al. (1978). *Introduction to population ecology*.
- ⁴⁷⁶ Iler, A. M., Compagnoni, A., Inouye, D. W., Williams, J. L., CaraDonna, P. J., Anderson, A., and
⁴⁷⁷ Miller, T. E. (2019). Reproductive losses due to climate change-induced earlier flowering are
⁴⁷⁸ not the primary threat to plant population viability in a perennial herb. *Journal of Ecology*,
⁴⁷⁹ 107(4):1931–1943.
- ⁴⁸⁰ Jones, M. H., Macdonald, S. E., and Henry, G. H. (1999). Sex-and habitat-specific responses
⁴⁸¹ of a high arctic willow, *salix arctica*, to experimental climate change. *Oikos*, pages 129–138.
- ⁴⁸² Karger, D. N., Conrad, O., Böhner, J., Kawohl, T., Kreft, H., Soria-Auza, R. W., Zimmermann,
⁴⁸³ N. E., Linder, H. P., and Kessler, M. (2017). Climatologies at high resolution for the earth's
⁴⁸⁴ land surface areas. *Scientific data*, 4(1):1–20.
- ⁴⁸⁵ Kindiger, B. (2004). Interspecific hybrids of *poa arachnifera* × *poa secunda*. *Journal of New*
⁴⁸⁶ *Seeds*, 6(1):1–26.
- ⁴⁸⁷ Knight, T. M., Steets, J. A., Vamosi, J. C., Mazer, S. J., Burd, M., Campbell, D. R., Dudash,
⁴⁸⁸ M. R., Johnston, M. O., Mitchell, R. J., and Ashman, T.-L. (2005). Pollen limitation of plant
⁴⁸⁹ reproduction: pattern and process. *Annu. Rev. Ecol. Evol. Syst.*, 36:467–497.
- ⁴⁹⁰ Konapala, G., Mishra, A. K., Wada, Y., and Mann, M. E. (2020). Climate change will affect
⁴⁹¹ global water availability through compounding changes in seasonal precipitation and
⁴⁹² evaporation. *Nature communications*, 11(1):3044.

- 493 Kremer, A., Ronce, O., Robledo-Arnuncio, J. J., Guillaume, F., Bohrer, G., Nathan, R., Bridle,
494 J. R., Gomulkiewicz, R., Klein, E. K., Ritland, K., et al. (2012). Long-distance gene flow and
495 adaptation of forest trees to rapid climate change. *Ecology letters*, 15(4):378–392.
- 496 Lee-Yaw, J. A., Kharouba, H. M., Bontrager, M., Mahony, C., Csergő, A. M., Noreen, A. M.,
497 Li, Q., Schuster, R., and Angert, A. L. (2016). A synthesis of transplant experiments and
498 ecological niche models suggests that range limits are often niche limits. *Ecology letters*,
499 19(6):710–722.
- 500 Leicht-Young, S. A., Silander, J. A., and Latimer, A. M. (2007). Comparative performance of
501 invasive and native celastrus species across environmental gradients. *Oecologia*, 154:273–282.
- 502 Liaw, A., Wiener, M., et al. (2002). Classification and regression by randomforest. *R news*,
503 2(3):18–22.
- 504 Louthan, A. M., Keighron, M., Kiekebusch, E., Cayton, H., Terando, A., and Morris, W. F.
505 (2022). Climate change weakens the impact of disturbance interval on the growth rate of
506 natural populations of venus flytrap. *Ecological Monographs*, 92(4):e1528.
- 507 Maguire Jr, B. (1973). Niche response structure and the analytical potentials of its relationship
508 to the habitat. *The American Naturalist*, 107(954):213–246.
- 509 McLean, N., Lawson, C. R., Leech, D. I., and van de Pol, M. (2016). Predicting when climate-
510 driven phenotypic change affects population dynamics. *Ecology Letters*, 19(6):595–608.
- 511 Merow, C., Bois, S. T., Allen, J. M., Xie, Y., and Silander Jr, J. A. (2017). Climate change both
512 facilitates and inhibits invasive plant ranges in new england. *Proceedings of the National
513 Academy of Sciences*, 114(16):E3276–E3284.
- 514 Miller, T. and Compagnoni, A. (2022a). Data from: Two-sex demography, sexual niche
515 differentiation, and the geographic range limits of texas bluegrass (*Poa arachnifera*). *American
516 Naturalist, Dryad Digital Repository*. <https://doi.org/10.5061/dryad.kkwh70s5x>.
- 517 Miller, T. E. and Compagnoni, A. (2022b). Two-sex demography, sexual niche differentiation,
518 and the geographic range limits of texas bluegrass (*poa arachnifera*). *The American
519 Naturalist*, 200(1):17–31.
- 520 Morrison, C. A., Robinson, R. A., Clark, J. A., and Gill, J. A. (2016). Causes and consequences
521 of spatial variation in sex ratios in a declining bird species. *Journal of Animal Ecology*,
522 85(5):1298–1306.

- 523 Morrison, S. F. and Hik, D. S. (2007). Demographic analysis of a declining pika *ochotona*
524 *collaris* population: linking survival to broad-scale climate patterns via spring snowmelt
525 patterns. *Journal of Animal ecology*, pages 899–907.
- 526 Nomoto, H. A. and Alexander, J. M. (2021). Drivers of local extinction risk in alpine plants
527 under warming climate. *Ecology Letters*, 24(6):1157–1166.
- 528 O'Connell, R. D., Doak, D. F., Horvitz, C. C., Pasarella, J. B., and Morris, W. F. (2024). Nonlinear
529 life table response experiment analysis: Decomposing nonlinear and nonadditive population
530 growth responses to changes in environmental drivers. *Ecology Letters*, 27(3):e14417.
- 531 Pease, C. M., Lande, R., and Bull, J. (1989). A model of population growth, dispersal and
532 evolution in a changing environment. *Ecology*, 70(6):1657–1664.
- 533 Petry, W. K., Soule, J. D., Iler, A. M., Chicas-Mosier, A., Inouye, D. W., Miller, T. E., and
534 Mooney, K. A. (2016). Sex-specific responses to climate change in plants alter population
535 sex ratio and performance. *Science*, 353(6294):69–71.
- 536 Piironen, J. and Vehtari, A. (2017). Comparison of bayesian predictive methods for model
537 selection. *Statistics and Computing*, 27:711–735.
- 538 Pottier, P., Burke, S., Drobniak, S. M., Lagisz, M., and Nakagawa, S. (2021). Sexual (in) equality?
539 a meta-analysis of sex differences in thermal acclimation capacity across ectotherms.
540 *Functional Ecology*, 35(12):2663–2678.
- 541 Pulliam, H. R. (2000). On the relationship between niche and distribution. *Ecology letters*,
542 3(4):349–361.
- 543 Reed, P. B., Peterson, M. L., Pfeifer-Meister, L. E., Morris, W. F., Doak, D. F., Roy, B. A., Johnson,
544 B. R., Bailes, G. T., Nelson, A. A., and Bridgman, S. D. (2021). Climate manipulations
545 differentially affect plant population dynamics within versus beyond northern range limits.
546 *Journal of Ecology*, 109(2):664–675.
- 547 Sanderson, B. M., Knutti, R., and Caldwell, P. (2015). A representative democracy to reduce
548 interdependency in a multimodel ensemble. *Journal of Climate*, 28(13):5171–5194.
- 549 Sasaki, M., Hedberg, S., Richardson, K., and Dam, H. G. (2019). Complex interactions
550 between local adaptation, phenotypic plasticity and sex affect vulnerability to warming
551 in a widespread marine copepod. *Royal Society open science*, 6(3):182115.

- 552 Schultz, E. L., Hülsmann, L., Pillet, M. D., Hartig, F., Breshears, D. D., Record, S., Shaw, J. D.,
553 DeRose, R. J., Zuidema, P. A., and Evans, M. E. (2022). Climate-driven, but dynamic and
554 complex? a reconciliation of competing hypotheses for species' distributions. *Ecology letters*,
555 25(1):38–51.
- 556 Schwalm, C. R., Glendon, S., and Duffy, P. B. (2020). Rcp8. 5 tracks cumulative co2 emissions.
557 *Proceedings of the National Academy of Sciences*, 117(33):19656–19657.
- 558 Schwinning, S., Lortie, C. J., Esque, T. C., and DeFalco, L. A. (2022). What common-garden
559 experiments tell us about climate responses in plants.
- 560 Sexton, J. P., McIntyre, P. J., Angert, A. L., and Rice, K. J. (2009). Evolution and ecology of
561 species range limits. *Annu. Rev. Ecol. Evol. Syst.*, 40:415–436.
- 562 Sherry, R. A., Zhou, X., Gu, S., Arnone III, J. A., Schimel, D. S., Verburg, P. S., Wallace,
563 L. L., and Luo, Y. (2007). Divergence of reproductive phenology under climate warming.
564 *Proceedings of the National Academy of Sciences*, 104(1):198–202.
- 565 Sletvold, N. and Ågren, J. (2015). Climate-dependent costs of reproduction: Survival and
566 fecundity costs decline with length of the growing season and summer temperature.
567 *Ecology Letters*, 18(4):357–364.
- 568 Sletvold, N., Dahlgren, J. P., Øien, D.-I., Moen, A., and Ehrlén, J. (2013). Climate warming
569 alters effects of management on population viability of threatened species: results from
570 a 30-year experimental study on a rare orchid. *Global Change Biology*, 19(9):2729–2738.
- 571 Smith, M. D., Wilkins, K. D., Holdrege, M. C., Wilfahrt, P., Collins, S. L., Knapp, A. K., Sala,
572 O. E., Dukes, J. S., Phillips, R. P., Yahdjian, L., et al. (2024). Extreme drought impacts have
573 been underestimated in grasslands and shrublands globally. *Proceedings of the National
574 Academy of Sciences*, 121(4):e2309881120.
- 575 Stan Development Team (2023). RStan: the R interface to Stan. R package version 2.21.8.
- 576 Thomson, A. M., Calvin, K. V., Smith, S. J., Kyle, G. P., Volke, A., Patel, P., Delgado-Arias,
577 S., Bond-Lamberty, B., Wise, M. A., Clarke, L. E., et al. (2011). Rcp4. 5: a pathway for
578 stabilization of radiative forcing by 2100. *Climatic change*, 109:77–94.
- 579 Tognetti, R. (2012). Adaptation to climate change of dioecious plants: does gender balance
580 matter? *Tree Physiology*, 32(11):1321–1324.

- 581 Villellas, J., Doak, D. F., García, M. B., and Morris, W. F. (2015). Demographic compensation
582 among populations: what is it, how does it arise and what are its implications? *Ecology*
583 letters, 18(11):1139–1152.
- 584 Welbergen, J. A., Klose, S. M., Markus, N., and Eby, P. (2008). Climate change and the
585 effects of temperature extremes on australian flying-foxes. *Proceedings of the Royal Society*
586 *B: Biological Sciences*, 275(1633):419–425.
- 587 Williams, J. L., Jacquemyn, H., Ochocki, B. M., Brys, R., and Miller, T. E. (2015). Life
588 history evolution under climate change and its influence on the population dynamics of
589 a long-lived plant. *Journal of Ecology*, 103(4):798–808.
- 590 Zhao, H., Li, Y., Zhang, X., Korpelainen, H., and Li, C. (2012). Sex-related and stage-dependent
591 source-to-sink transition in populus cathayana grown at elevated co₂ and elevated
592 temperature. *Tree Physiology*, 32(11):1325–1338.

Supporting Information

593 S.1 XX

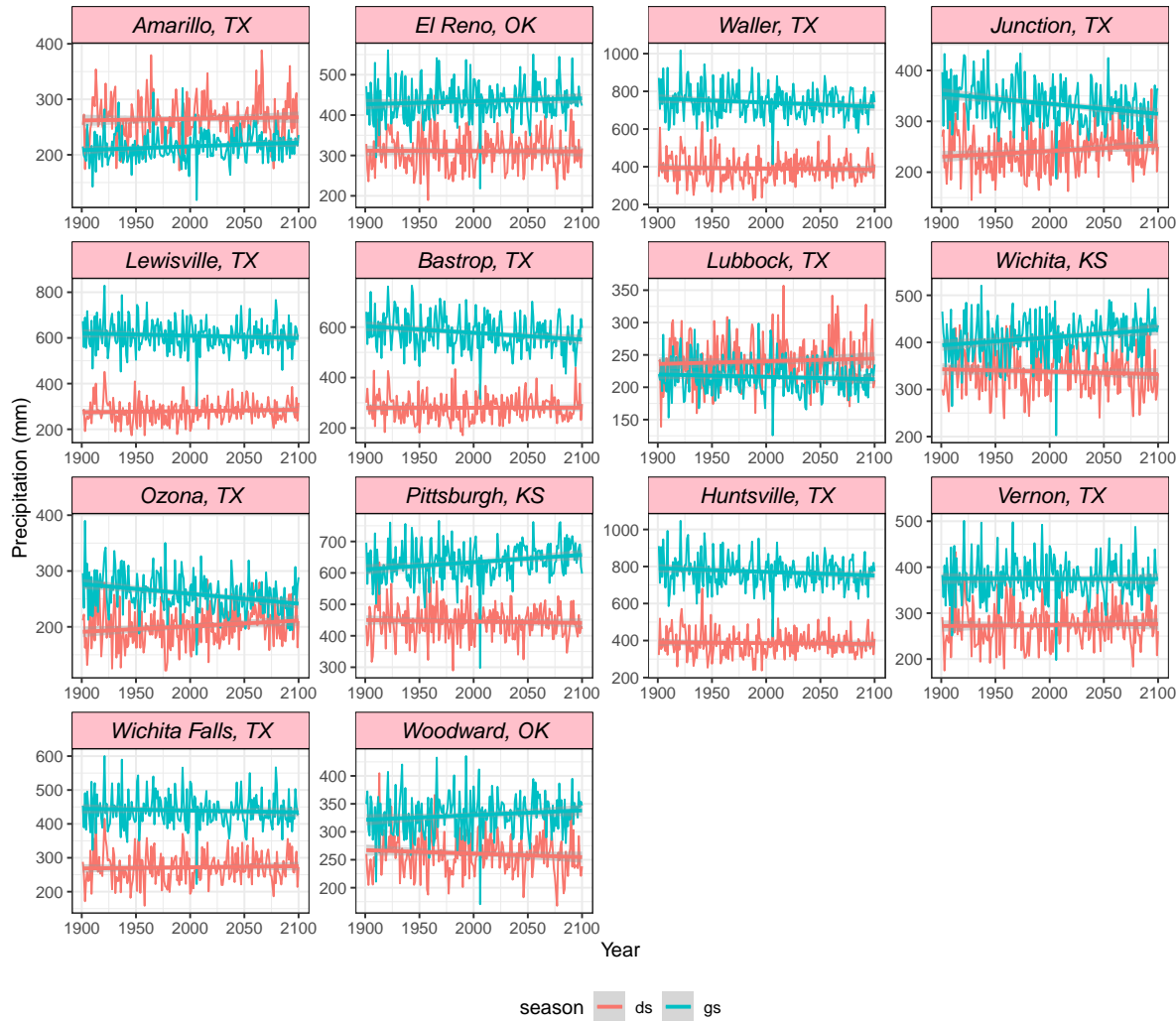


Figure S-1: Precipitation variation accross the study sites from 1990 to 2100

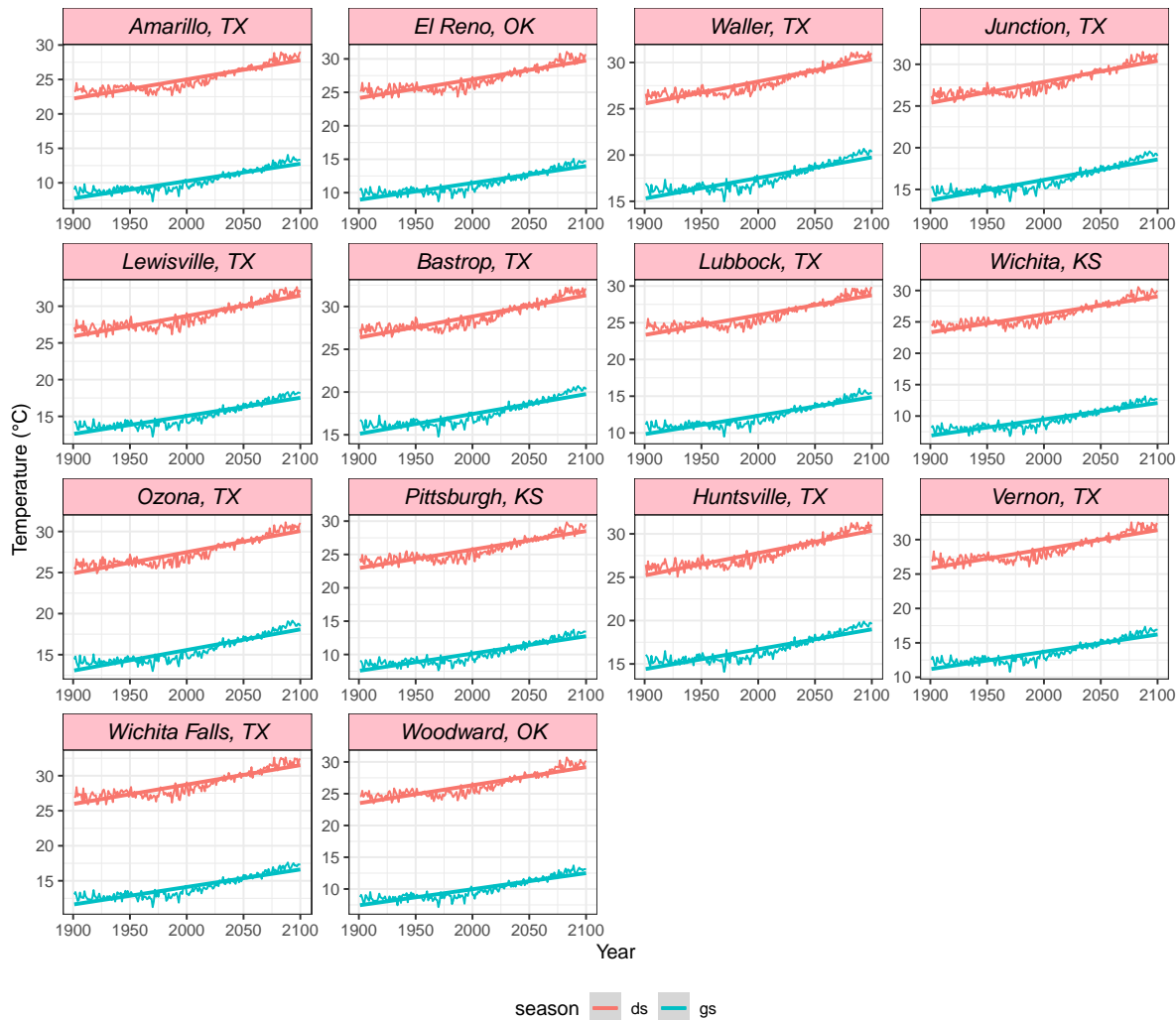


Figure S-2: Temperature variation accross the study sites from 1990 to 2100

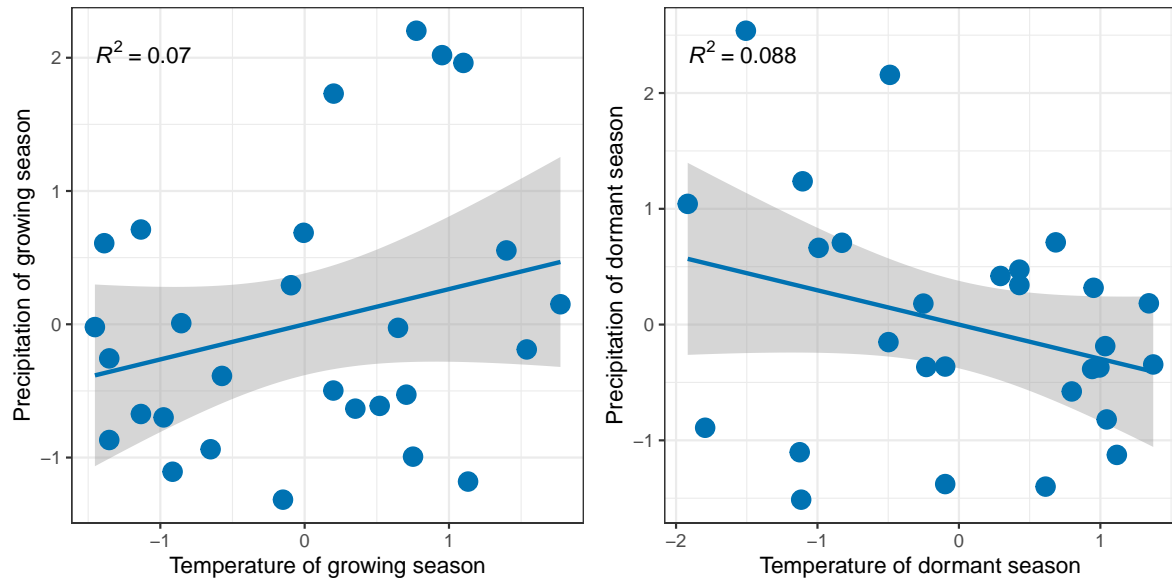


Figure S-3: Relation between precipitation and temperature for each season (growing and dormant). R^2 indicates the value of proportion of explained variance between the temperature and precipitation

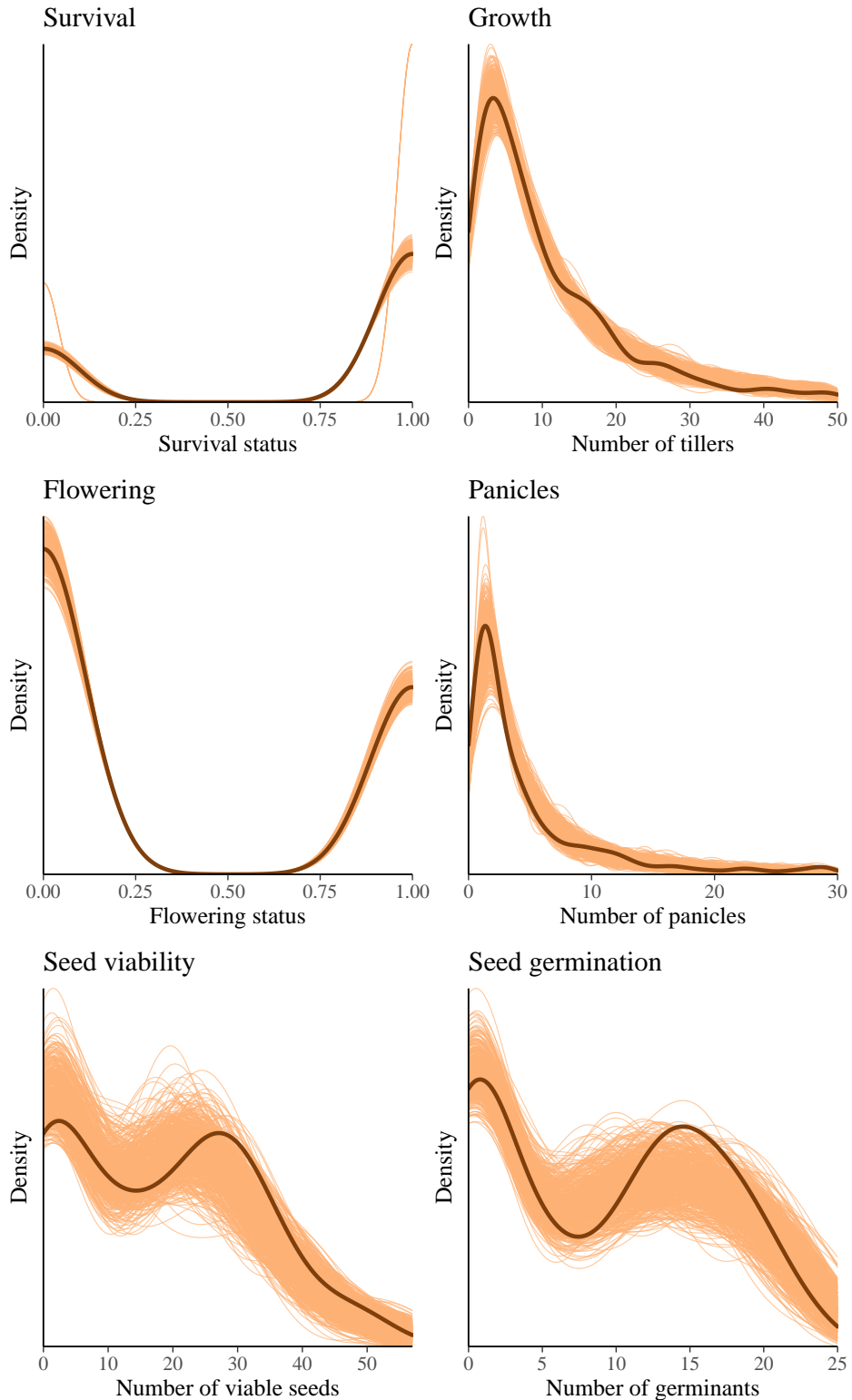


Figure S-4: Consistency between real data and simulated values suggests that the fitted model accurately describes the data. Graph shows density curves for the observed data (light blue) along with the simulated values (dark blue). The first column shows the linear models and the second column shows the 2 degree polynomial models.

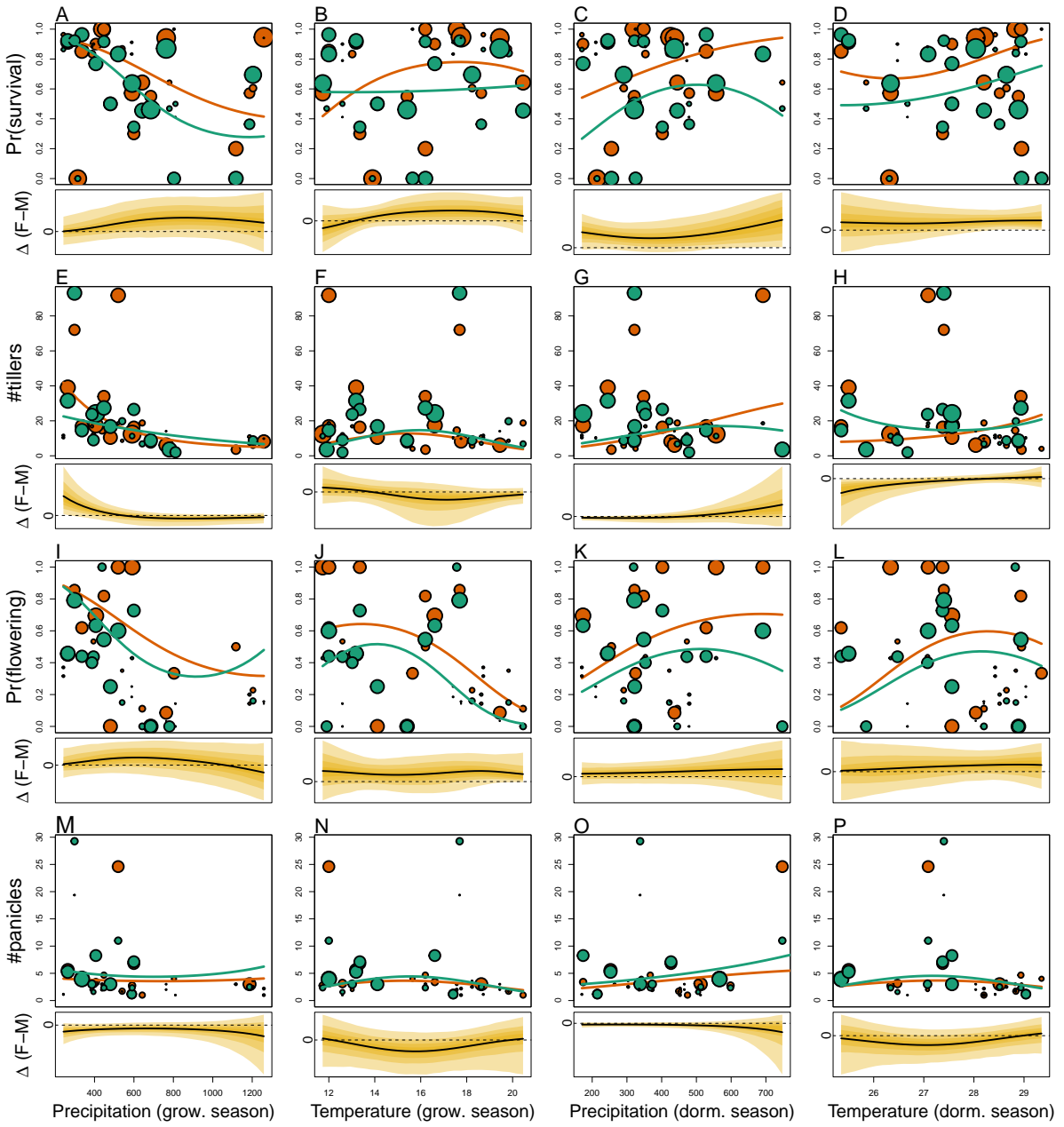


Figure S-5: Sex specific demographic response to climate across species range: A–D, seasonal probability of survival; E–H, seasonal growth (change in number of tillers); I–L, seasonal probability of flowering; M–P, number of panicles produced given flowering. Points show means by site for females (orange) and males (green). Points sizes are proportional to the sample sizes of the mean and are jittered. Lines show fitted statistical models for females (orange) and males (green) based on posterior mean parameter values. Lower panels below each data panel show the posterior distribution of the difference between females and males as a function of climate (positive and negative values indicate female and male advantage, respectively); dashed horizontal line shows zero difference.

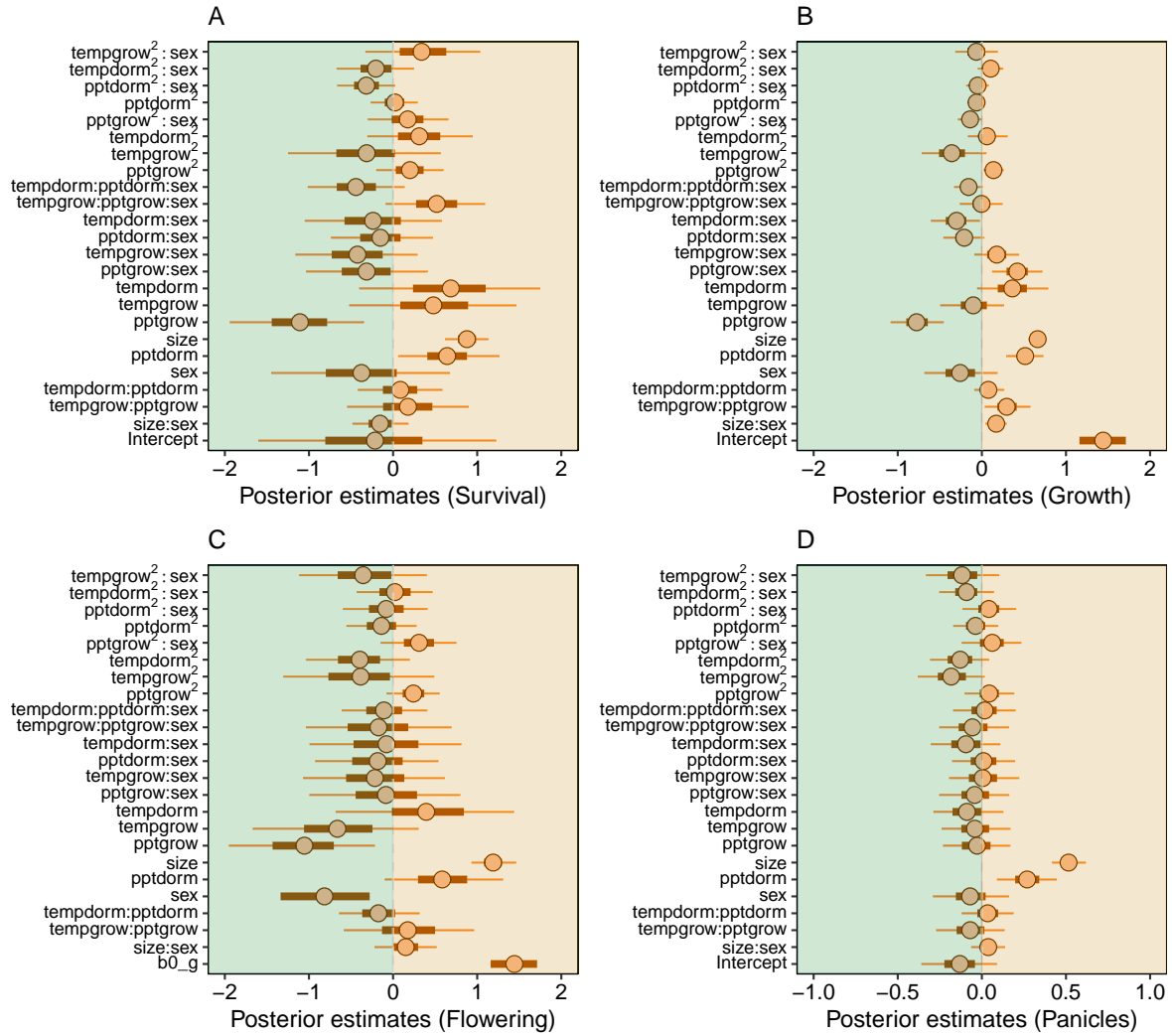


Figure S-6: Mean parameter values and 95% credible intervals for all vital rates.

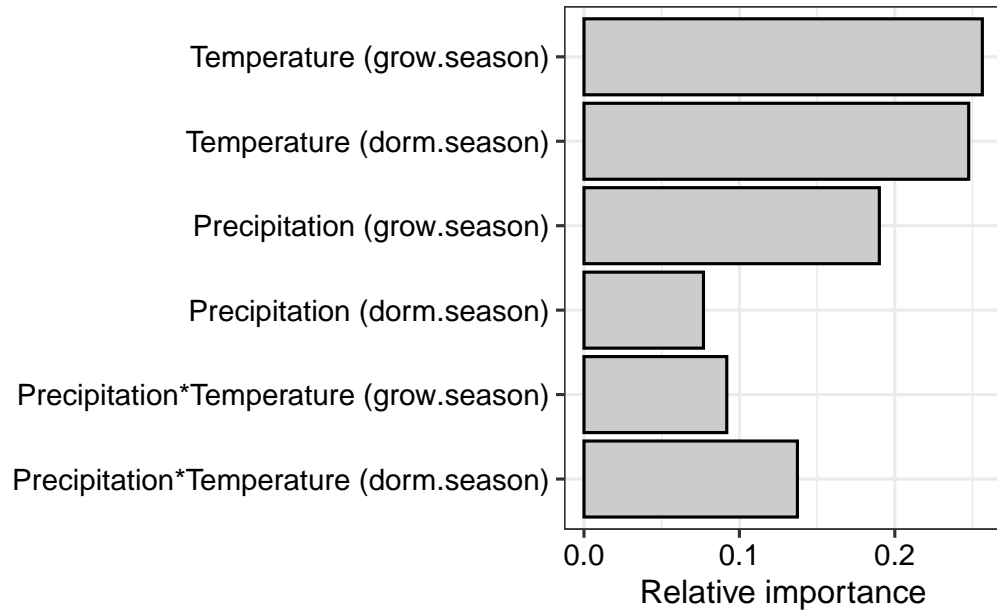


Figure S-7: XXX

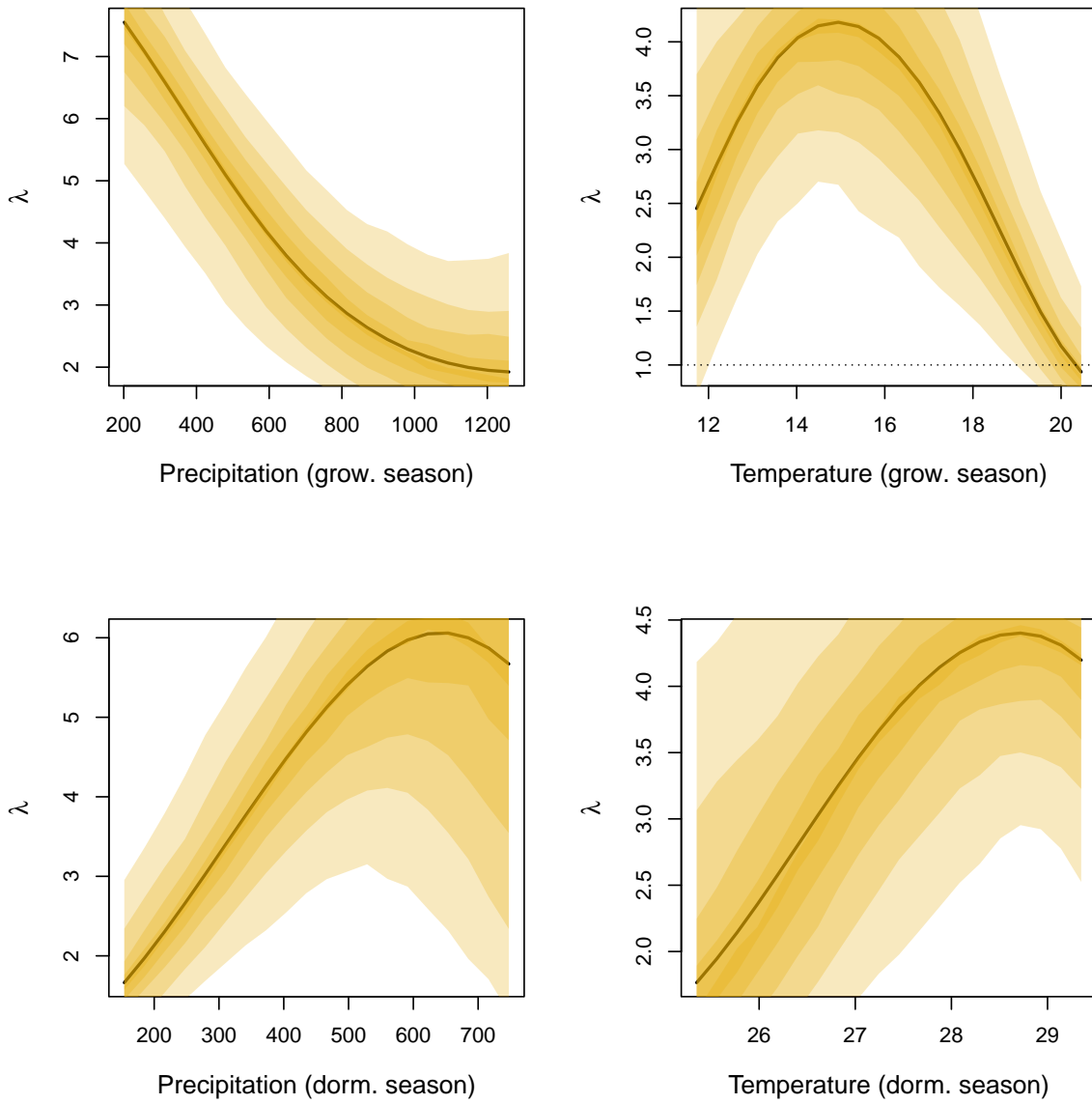


Figure S-8: Population growth rate (λ) as a function of seasonal climate (2016-2017), predicted by the two-sex matrix projection model that incorporates sex-specific demographic responses to climate with sex ratio-dependent seed fertilization. We show the mean posterior distribution of λ in solid lines, and the 5, 25, 50, 75, and 95% percentiles of parameter uncertainty in shaded gold color. The dashed horizontal line indicates the limit of population viability ($\lambda = 1$)

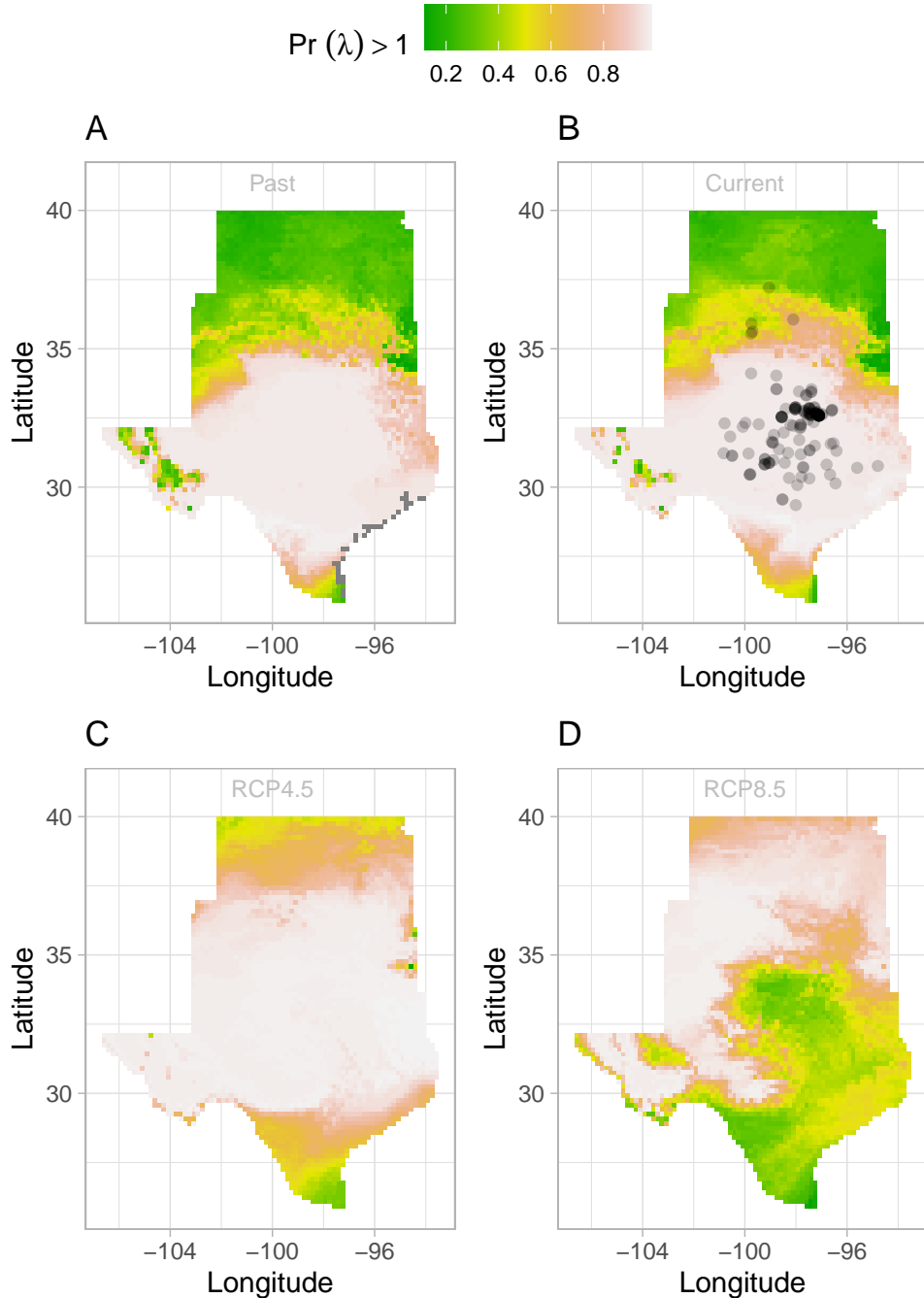


Figure S-9: Past (A), Current (B), Future CMCM (2070–20100) (C and D) predicted range shift based on population growth rate. Future projections were based on the average population growth rate in four CES. The black circles on panel B indicate all known presence points collected from GBIF from 1990 to 2019, which corresponds to the current condition in our prediction. The occurrences of GBIFs are distributed in with higher population fitness habitat ($\lambda > 1$), confirming that our study approach can reasonably predict range shifts.

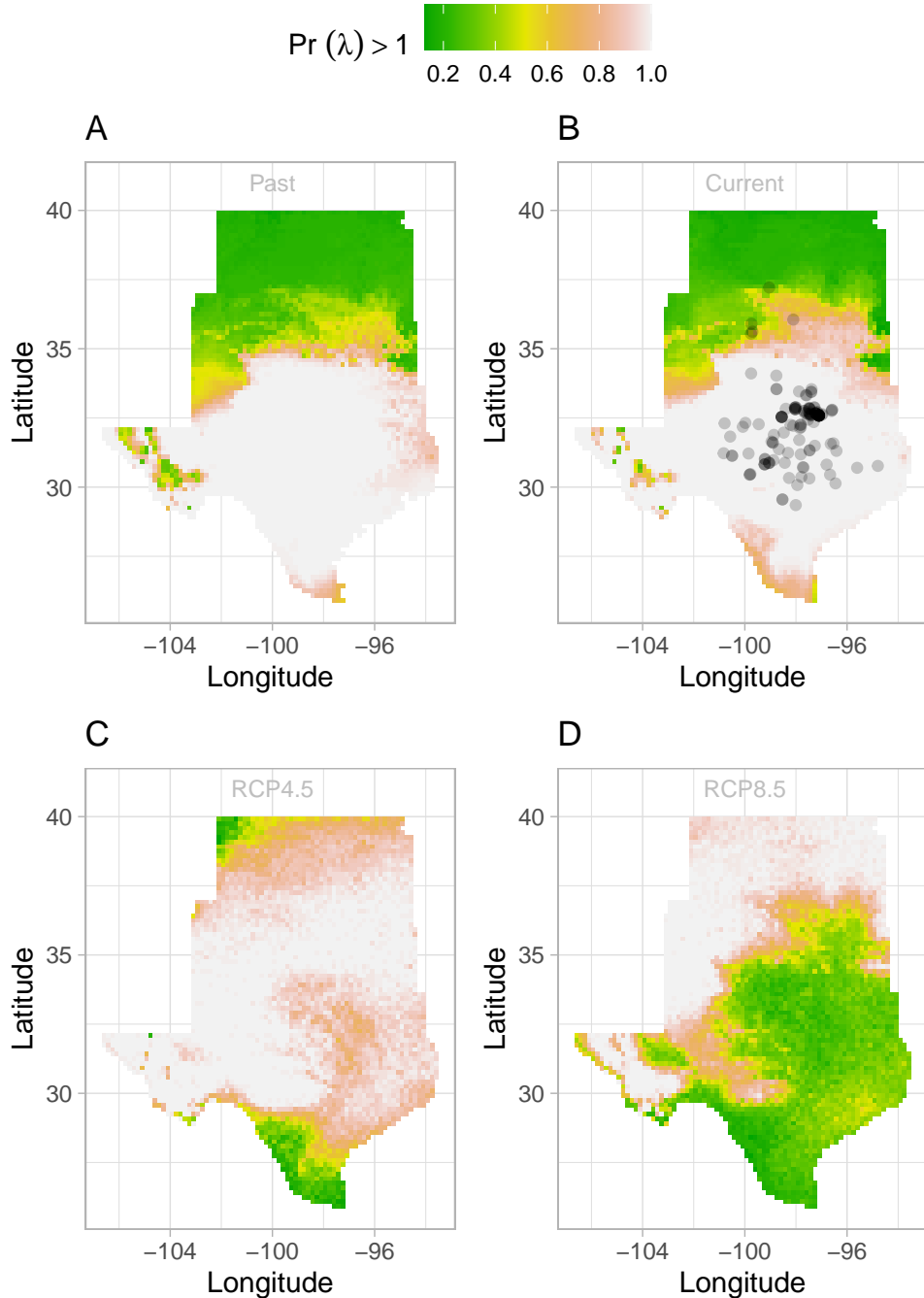


Figure S-10: Past (A), Current (B), Future CMCM (2070–20100) (C and D) predicted range shift based on population growth rate. Future projections were based on the average population growth rate in four CES. The black circles on panel B indicate all known presence points collected from GBIF from 1990 to 2019, which corresponds to the current condition in our prediction. The occurrences of GBIFs are distributed in with higher population fitness habitat ($\lambda > 1$), confirming that our study approach can reasonably predict range shifts.

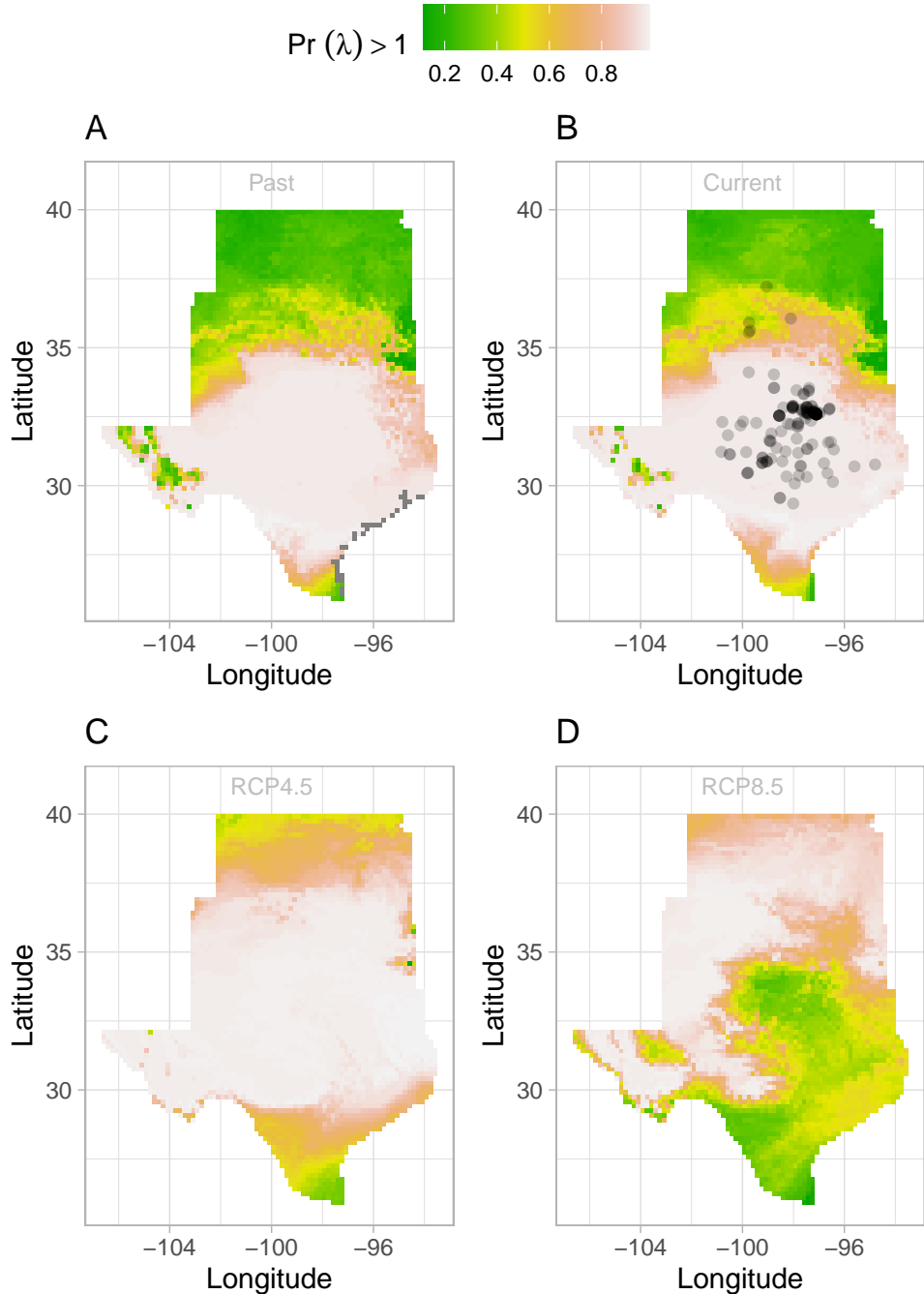


Figure S-11: Past (A), Current (B), Future CMCM (2070–20100) (C and D) predicted range shift based on population growth rate. Future projections were based on the average population growth rate in four ACC. The black circles on panel B indicate all known presence points collected from GBIF from 1990 to 2019, which corresponds to the current condition in our prediction. The occurrences of GBIFs are distributed in with higher population fitness habitat ($\lambda > 1$), confirming that our study approach can reasonably predict range shifts.

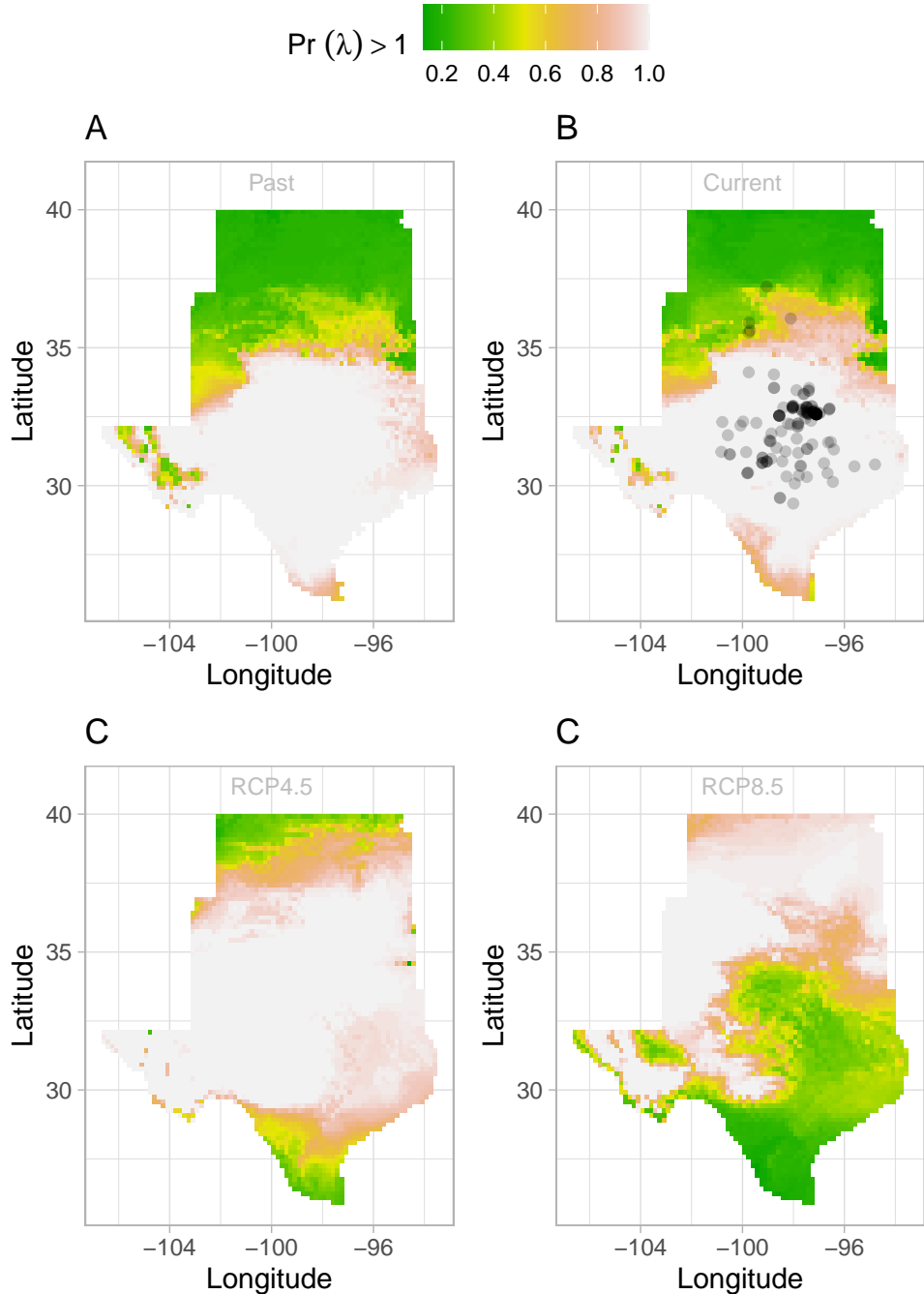


Figure S-12: Past (A), Current (B), Future ACCESS (2070–20100) (C and D) predicted range shift based on population growth rate suing the female dominat model. Future projections were based on the average population growth rate in four GCMs. The black circles on panel B indicate all known presence points collected from GBIF from 1990 to 2019, which corresponds to the current condition in our prediction. The occurrences of GBIFs are distributed inwith higher population fitness habitat ($\lambda > 1$) , confirming that our study approach can reasonably predict range shifts.

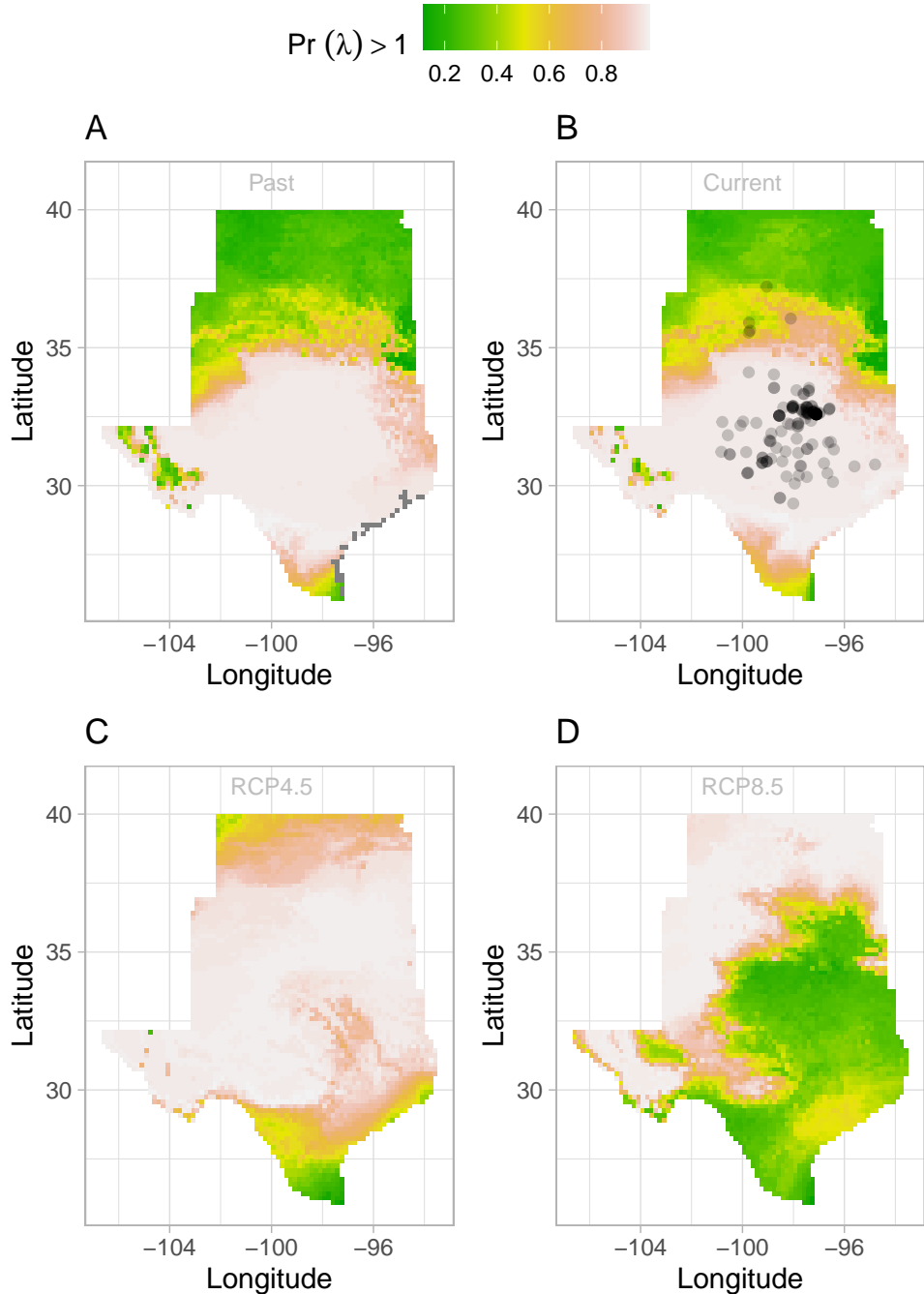


Figure S-13: Past (A), Current (B), Future MIROC (2070–20100) (C and D) predicted range shift based on population growth rate. Future projections were based on the average population growth rate in four ACC. The black circles on panel B indicate all known presence points collected from GBIF from 1990 to 2019, which corresponds to the current condition in our prediction. The occurrences of GBIFs are distributed in with higher population fitness habitat ($\lambda > 1$), confirming that our study approach can reasonably predict range shifts.

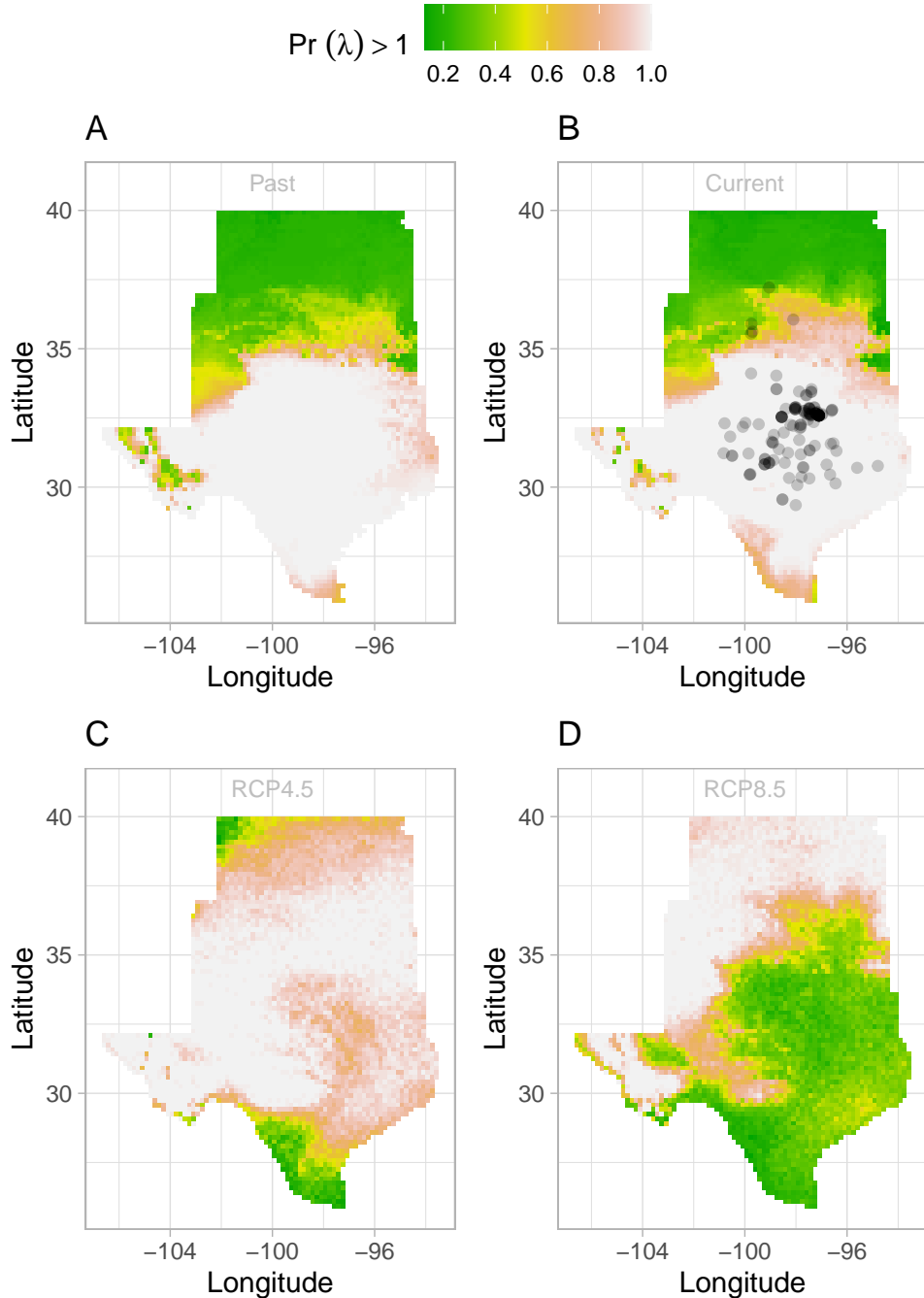


Figure S-14: Past (A), Current (B), Future CMCM (2070–20100) (C and D) predicted range shift based on population growth rate. Future projections were based on the average population growth rate in four ACC. The black circles on panel B indicate all known presence points collected from GBIF from 1990 to 2019, which corresponds to the current condition in our prediction. The occurrences of GBIFs are distributed in with higher population fitness habitat ($\lambda > 1$), confirming that our study approach can reasonably predict range shifts.

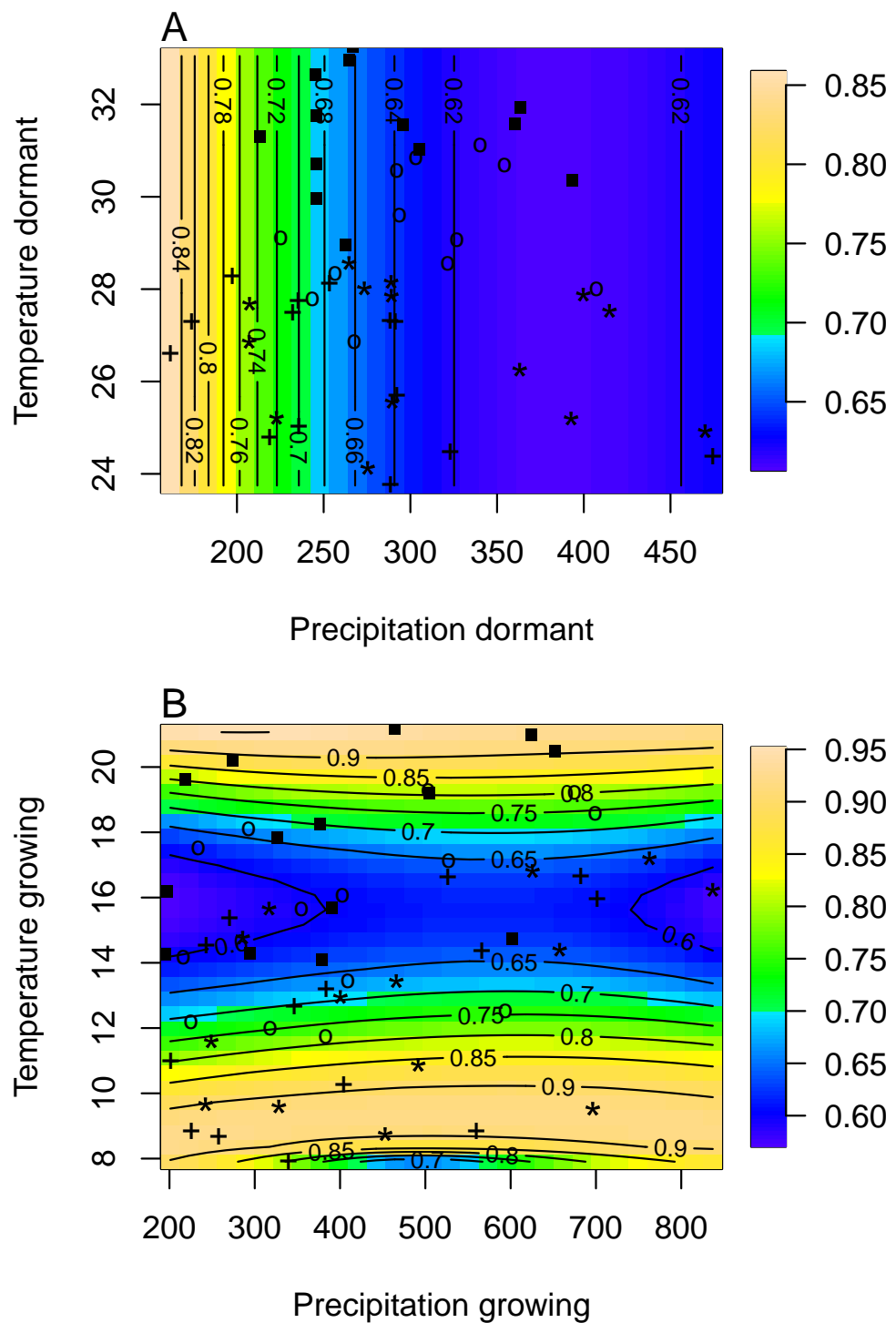


Figure S-15: XXX

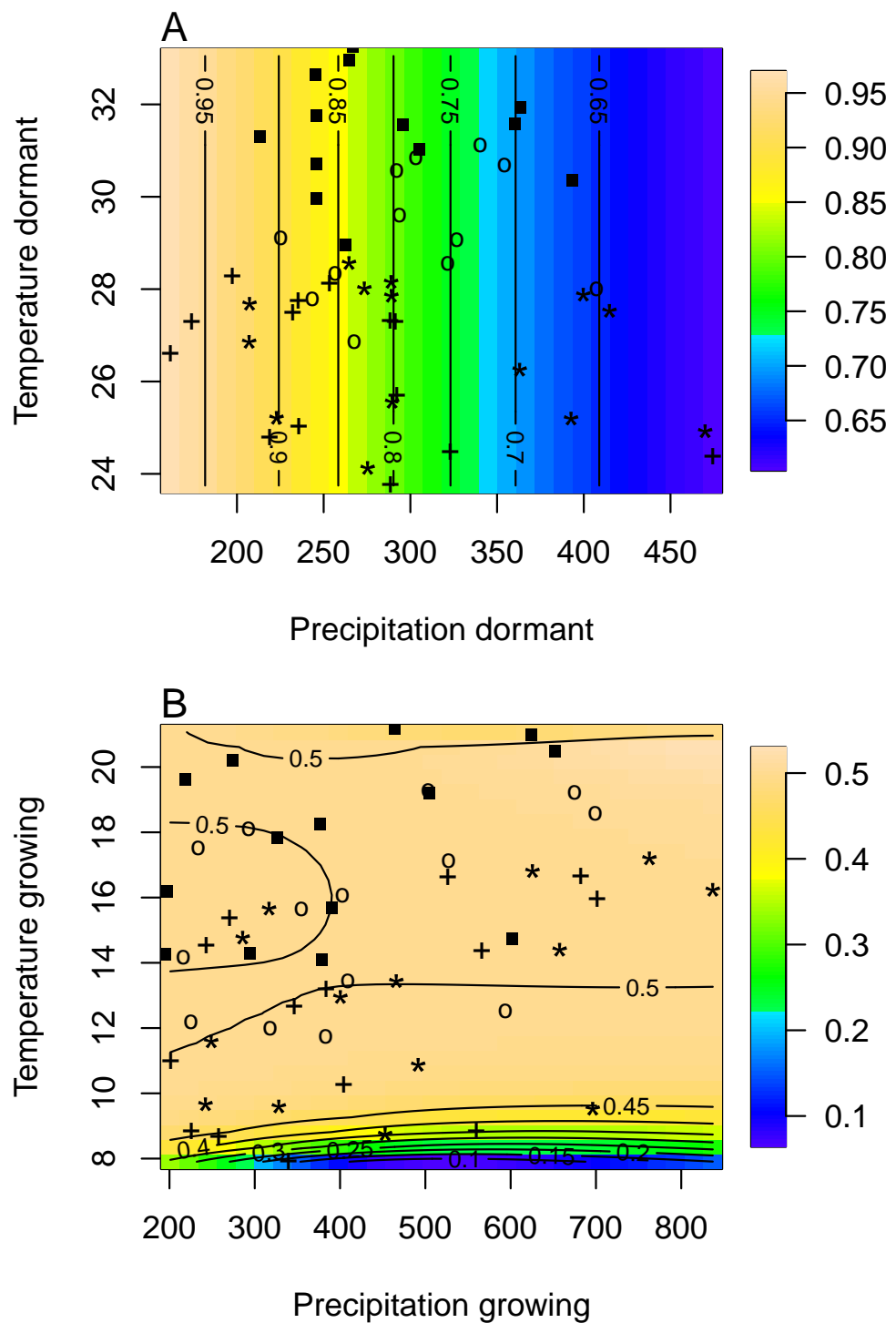


Figure S-16: XXX